NUMERICAL INVESTIGATION OF SEISMIC ISOLATION FOR TALL CLT BUILDINGS

By

VINCENT BORDRY

A thesis submitted in partial fulfillment of the
requirements for the degree of

MASTER OF SCIENCE IN CIVIL ENGINEERING

WASHINGTON STATE UNIVERSITY
Department of Civil & Environmental Engineering

MAY 2014

©Copyright by VINCENT BORDRY, 2014
All Rights Reserved

To the Faculty of Washington State University:

The members of the Committee appointed to examine the thesis of VINCENT BORDRY find it satisfactory and recommend that it be accepted.

_____
James D. Dolan, Ph.D., Chair

_____
Donald A. Bender, Ph.D.

_____
Marjan Popovski, Ph.D.

ACKNOWLEDGMENT

I am grateful to my advisor Dr Dolan for is continuous assistance during my stay at Washington State University. The completion of this thesis would not have been possible whiteout his tremendous support and his innovative view of the mechanical concepts studied.

I would like to also thank committees' members Dr Bender and Dr Popovski. They have continuously been helpful and their comments were always valuable.

I would like to thank Mrs. Ruddick for here guidance during the completion of my program. She has always been very caring and effective to help solving any problem.

Finally, I thank my parents for their constant support and Khoi Mai, my office mate for his assistance and company.

NUMERICAL INVESTIGATION OF SEISMIC ISOLATION FOR

TALL CLT BUILDINGS

Abstract

By Vincent Bordry, M.S.
Washington State University
May 2014

Chair: James D. Dolan

The increasing concern for structure resiliency in seismic regions has brought up the need for new innovative isolation systems to reduce the accelerations in upper stories and protect the structure from significant damage. The objective of this thesis is to study different configurations of seismic isolation; their effects compare to a non-isolated model are evaluated. The isolators are springs and dampers that connect the stories together. Isolate the first story from the rest of the building has the most impact in reducing the force demands on the structure. Isolate more stories mostly increase the natural period of the building and lower the force demands in the isolators. The stiffness and damping coefficient of the isolators are also estimated.

Skyscrapers are usually complex to model and require significant computational effort. To be able to compare several configurations, it is necessary to have a model that can be run in a short time but with a reasonable accuracy. A modeling technique that uses ABAQUS V6 (2011)'s substructuring tool to compare different isolation systems with a reasonable computational effort is presented. A time-history analysis of a linear 10-story model during a 20 second event can be computed in less than 8 hours.

TABLE OF CONTENTS

LIST OF FIGURES

LIST OF TABLES

I. Introduction

The idea of a wood-based ”skyscraper” has emerged with the development of the Cross Laminated Timber (CLT) product. Associated with connectors and other materials, CLT seems to be very efficient in high-rise buildings (Ceccotti, Sandhaas, & Yasumura, 2010). The magnitude of loads involved here are much larger compared to the usual applications of wood-based materials so that the behavior of CLT is hard to predict. In order to meet the earthquake code’s requirements, the structure must show the ability to resist lateral forces. In tall buildings, base isolation is probably the best way to meet these requirements. In base isolation, larges rubber isolators support buildings and absorb the seismic forces. For CLT a distributed base isolation might be more appropriate. By keeping this modular aspect, the construction time is not affected.

Traditional seismic design allows a structure to deform plastically during a major event. The inclusion of nonlinear effects is then of great interest when modeling a skyscraper during an earthquake event. It results in higher accuracy and better performance of the final design, but considerably increase the computation time. For isolated structures, experiences have shown that the demand above the isolation level is significantly reduced. The plastic deformations are then less important and a linear dynamic analysis becomes appropriate when modeling this system.

Ryan & Earl (2010) conclude that configurations, where the first floors are isolated provide the best results. As there are an important number of configurations possible, it is essential to have a reasonable computation time to consider most of these configurations. The computation time has been a driving factor during the development of the model used in this

investigation. The use of substructures in dynamic linear analysis brings additional approximation, but considerably reduces the computational time.

The objectives of this research are, first to develop a modeling approach of vertically distributed base isolation on the response of tall CLT buildings. Secondly, to estimate the story forces and displacements for different damping, restoring spring values, and number of stories activated to help decide which provides the best performances. The first section of the thesis proposes a technique to model the different elements with ABAQUS V6 (2011). Thanks to different tools brought by ABAQUS V6 (2011), it was possible to reach a high level of details to the structure. In the second section, the assembly of the models is explained. Two intermediate models have been used to build the final skyscraper model. The first one is a shear wall model that is used to investigate the size effects of the wall panels. The second model is a model of a single story. This model is used as a part in the skyscraper model. Finally the results of the building response analysis are presented.

II. Literature review

A. Cross Laminated Timber (CLT)

Wood has always been a very practical and well-adapted material for humans use. We have quickly understood the need to transform or adapt the wood to get better performance. The last century has seen the development of new wood-based products dedicated to building construction. Those products have better structural capacity than untransformed wood.

Wood is an orthotropic material. This results in weaknesses when load is applied in certain directions, such as perpendicular to the grain. Trees, during their life, are also extremely influenced by the environment. The quality of the wood is then dependent of various parameters, such as location, species, and temperature. The first objective of developing wood composites is to reduce the tropicity. A more uniform product has more predictable mechanical capacities. The performance of these new products surpassed the expectation and the demand rapidly increased.

CLT is one of these promising construction materials. It was first developed in the 1990's in Switzerland, and since this time, the interest for this product has not decreased. CLT is made of layers of dimensional lumber that are glued together in layers, with the grain of each layer oriented at right angles. The most used wood species group for CLT is Spruce-Pine-Fir (Spruce, Larch or Pine). Each layer is vertical or horizontal and is made of 1.5in. thick timber laminations. Theoretically, there is no limitation on the number of layers, but the three- or five- layers configurations are the most common. A photo of three- and five- layer CLT sections is presented in Figure 1.

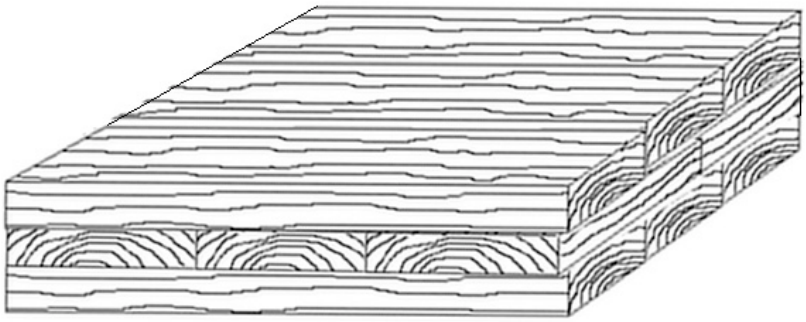

Figure 1: Three-layers CLT panels

1. Advantages of CLT

a) Structural

CLT has quickly shown an overall higher capacity compared to other engineered wood products. Engineered wood panels such as plywood or OSB are widely used in lateral force resisting system (LFRS). In this system the loads are transmitted to the surrounding shear wall and diaphragms through the connectors. The ability of the wood panel and the connectors to deform under the action of wind or earthquakes provides a very good energy dissipation capability. This soft behavior is interesting in small buildings and other configurations where the horizontal displacement is not a restrictive parameter. In tall buildings such as skyscrapers, a stiffer material is required to limit the displacement of the upper levels to a certain range. Concrete and steel are traditionally the materials used in tall buildings construction. CLT seems to be a good alternative between these traditional materials and wood light-frame construction. Used with properly designed connectors, CLT seems to be as stiff as concrete and makes the use of CLT in tall buildings possible (Van De Kuilen, Ceccotti, Xia, & He, 2011).

b) Others

As a wood based product, CLT has numerous advantages that natural fibers provide. The high concentration of water in cellulose gives a natural high thermal resistance to the wood. The density is also excellent; wood has the highest strength to weight ration of any material used in construction. The poor fire resistance associated with light-frame construction, and the sensitiveness of the wood to the exterior conditions can be easily overcome by using heavier cross sections and treatments. The advantages of CLT are:

- Reduced construction time and cost. Panels are prefabricated, so the onsite assembly phase is very easy to complete. The low weight and cost of the raw material are the main assets.
- The final building has outstanding thermal capacities; there is almost no need for extra isolation. Due to the precision of the machines used in manufacture, the cut of CLT panels is extremely precise which results in excellent airtightness.
- The life cycle cost of the material is the greener of all the traditional construction materials. The wood traps CO2 during the tree growth and keeps it enclosed during its life as a panel. Due to its low density, fabrication and transportation phases are less energy consuming, and the panels can be easily transformed at the end of life compared to steel and concrete. These are the reasons why CLT has one the lowest carbon footprints.

The versatility of CLT seems to suit the demand for a new generation of multistory buildings.

B. Seismic design

It is only recently that the design procedures have been updated to take into account the special conditions that a structure undergoes during an earthquake. The need for a compromise between lateral strength and energy dissipation has been highlighted above. A stiff structure will experience very small drifts, but excessive accelerations can cause danger to occupants and damage to unsecured buildings content. The structure may survive but the cost in human life and in material products could be severe. In the other hand, a soft structure will be highly damaged. In most cases the destruction of the remaining structure and the construction of a new one will be cheaper than repairing a damaged structure after an earthquake (Filiatrault & Folz, Performance-Based Seismic Design of Wood framed Buildings, 2002). Currently different techniques exist to improve the structure's resistance.

1. Flexible braced frames

In steel structures, braced frames are very common to increase lateral strength. In seismic region, the energy dissipation can be provided by passive dampers mounted at the connections (Skup, 2001). There are two main kinds of passive dampers: viscous and friction. In viscous damper, the damping is provided by the displacement of the fluid in the cylinder. The slip of two rough surfaces in contact is the mechanism of damping in friction dampers. The friction damping is active only when the load is above a minimum limit. Friction dampers are more used in those structures because they are less expensive and suit better for those applications (Pall & Marsh, 1982). The downside of friction dampers is their poor recentering abilities, which limits the maximum displacement possible.

2. **Rocking walls**

The technique of self-centering systems, named rocking wall, is a method to accommodate panels' deformation during earthquakes. Rocking is the rotation of the shear wall around its center of rigidity. For stiff materials, the ability of the panel to rock reduces the deformation in the panel. Attached with ductile connectors, the system dissipates energy. During CLT wall testing, the panels have behaved as rigid body (Pei, Popovski, & Van de Lindt, 2012). This technique relies on the yielding of ductile fuse elements. After a severe earthquake, the building would still require some repairs.

3. **Base isolation**

An alternative philosophy emerged 50 years ago. It relies on the association of stiff construction materials and ductile energy dissipaters. "The technique mitigates the effects of an earthquake by essentially isolating the structure and its contents from potentially dangerous ground motion" (Ramallo, Johnson, & Spencer, 2002). Initially, the isolators were located only at the buildings base. Passive lead-rubber bearing systems or sliding systems were used to connect the structure to the foundation and they deformed during an earthquake. They are able to reduce the base shear by at least a factor of 5. It also suppresses the dynamic effect of irregularities and appendages (Skinner & McVerry, 1975). The design of these systems depends on the weight of the structure and the magnitude of the earthquake encountered in the area, but they are usually able to displace up to 3 feet. A gap must then be present between the bottom of the structure and the foundation to accommodate this displacement.

Each earthquake are different, the magnitude and the frequency as well as the location of the epicenter are never the same. Even if base isolation is widely approved in the civil engineering world, there are concerns for certain type of earthquakes. Earthquakes with large

displacements and long natural period can overcome the lead-rubber base isolation (Li, Li, Li, & Samali, 2013). Researches focus now on improving the system. More complex lead rubber and active devices are developed to help widen the frequency range. The new lead-rubber isolators have better horizontal flexibility and energy dissipation capabilities. The active dampers can be instantly controlled to shift the damping coefficient in the safe zone. These systems are the state-of-the-art of base isolation devices; they are reserved for critical structures. For residential tall CLT buildings, these systems would not be cost competitive.

4. Distributed "base" isolation

The concept of a vertically distributed isolation system arose from base isolation. Several isolators that connect the floors together replace the base isolators. Each isolated story has the ability to translate in the horizontal plane. This technique has several advantages over base isolation. First it seems more efficient; each isolator is designed for a smaller mass. They are then smaller and any type of devices such as passive or active dampers and springs can be used. Secondly, the installation process is easier, especially for retrofit applications. Finally there is no need for a gap or moat at the base of the building. "Eliminating the seismic gap at the base could be aesthetically and economically appealing" (Ryan & Earl, 2010). The concept of distributed base isolation is illustrated in Figure 2.

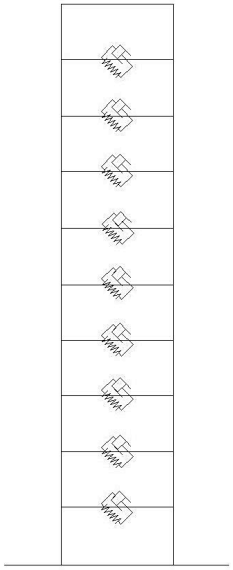

Figure 2: Concept of distributed isolation system

In their study of a 6-story isolated system, Ryan & Earl, demonstrated the effectiveness of different isolation systems. In their conclusions, they emphasized that a base isolated system behaved the same as a system with a first story isolated. Secondly, isolating the upper floor or the roof is the least efficient system. Finally, isolating the first few stories seems to result in the most efficient configurations. The benefice in terms of seismic demand reduction is smaller when compared to the base isolation configuration, but it could be a good technique to reduce the isolation capacities of the base. Stiffness and damping of the base isolators could be divided into two or more levels. Also, for the CLT configuration investigated in this study, the floor systems do not have to span significant distances as is typically done for base isolation systems since the CLT configuration will have virtually all of the floor area to transfer the gravity loads.

C. Finite element analysis (FEA) in civil engineering

The finite element analysis is a calculus method that gives numerical solution to field problems meaning that the solution is approximate. The approximation depends on the precision

of the model and the elements used. A field problem is any type of physical problem that can be described with differential equations.

1. Concepts of FEA

The structure is discretized in small pieces called “finite elements”. The behavior of each element, such as the modulus of elasticity or the thermal conduction, and the boundary conditions must be defined. The variation of the field quantities, are then estimated between each element. In mechanics, the differential equation is based on the principle of virtual work (PVW), and the fields quantities calculated are usually the stress or the strain. The number of degrees of freedom (DOF) of the element must also be decided. DOF defines the allowable motions of the element; in solid mechanic the DOFs are usually the translation and the rotation along 3 directions. The computation time depends on the number of elements and the element’s number of degrees of freedom.

2. ABAQUS V6 (2011) ®

For decades, finite element analysis has gained a very strong standing in numerical analysis. The first computer application was developed in the 1960’s. Nowadays, there is a lot of software that use the FEA. They are usually specialized in a certain type of application such as solid mechanics, fluid mechanics, thermodynamics, etc. The level of details available also differs; typically, the more expensive programs provide more detailed analysis capabilities.

One of the most famous finite element (FE) software programs is ABAQUS V6 (2011). It is probably the software with the widest range of applications and a very detailed library of tools and elements. It has initially developed for nonlinear analysis, and ABAQUS V6 (2011). is

efficient for this type of analysis. In mechanics, when it is expected to have a material that will deform in a plastic fashion; the nonlinear analysis is recommended.

There is actually no software that is dedicated to a general-purpose nonlinear analysis for large structures, but ABAQUS V6 (2011) is the only one to be able to solve large problems in nonlinear analysis (Lee, 2007).

III. Modeling techniques

A square of 100ft. with centered interior walls has been chosen for the building shape. The story height was taken as 10ft. The model is made of two main elements:

- panels, which represent the wall and the floor;
- connectors, which link the panels together.

The way of defining this material and its connectors is presented below.

A. Panels elements

1. Wood material definition

CLT is a wood-based product made of 1.5 in. thick laminations glued and stacked at right angles. The number of layers usually runs from 3 up to 7. The raw material for CLT is usually spruce, pine or larch at 12% moisture content. It is assumed here that the wood species used is spruce. Wood is defined as an orthotropic material (properties are symmetric along three planes). The three-dimensional elastic behavior has been found in the literature (Keunecke, Hering, & Niemz, 2008):

Table 1: Engineering wood constants

E_T (psf)	8,291,517.4	G_{LR} (psf)	12,886,312.9	ν_{LR}	0.018	ν_{RL}	0.36
E_L (psf)	267,333,558.7	G_{RT} (psf)	1,106,928.0	ν_{TR}	0.48	ν_{TR}	0.21
E_R (psf)	13,053,396.4	G_{LT} (psf)	12,259,749.9	ν_{TL}	0.45	ν_{TL}	0.014

Where E is the elastic modulus, G is the shear modulus and ν is the Poisson's ratio. T,L and R are the three orthotropic directions: tangential direction, longitudinal direction and radial direction as illustrated in Figure 3.

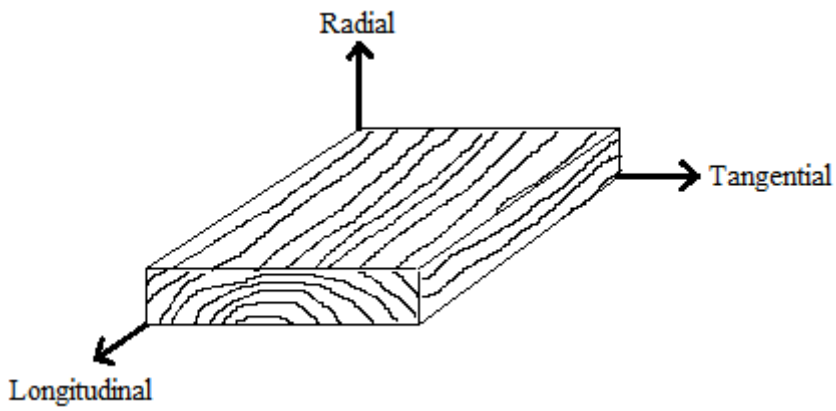

Figure 3: Orthotropic wood directions

Wood is stiffer in the direction of growth (longitudinal), the modulus of elasticity in that direction and the shear modulus in the plane normal to that direction are the highest. In ABAQUS V6 (2011), the material properties can be defined as a function of the 9 independent elastic stiffness parameters set into the stiffness tensor [D]. After manipulation and calculation, [D] is found to be:

Table 2: Stiffness tensor for orthotropic wood definition (psf)

14,710,863.3	263,265.1	3,184,056.7	0	0	0
263,265.1	8,457,233.7	4,274,702.8	0	0	0
3,184,056.7	4,274,702.8	301,333,063.8	0	0	0
0	0	0	12,259,765.0	0	0
0	0	0	0	1,106,929.4	0
0	0	0	0	0	12,886,328.8

The CLT handbook published by FPInnovations and Binational Softwood gives some guidelines on how to calculate the effective bending stiffness, EI_{eff}, of the layup as

$$EI_{eff} = \sum_{i=1}^{n} (E_i . b_i . \frac{h_i^3}{12}) + \sum_{i=1}^{n} (E_i . A_i . z_i^2)$$

where n is the number of plies, E_i is the modulus of elasticity of ply i, b_i is the width of ply i, h_i is the thickness of ply i and z_i the distance between the centroid of the ply and the neutral axis. The effective bending stiffness of the layup used for the wall element is found to be $EI_{eff} = 402.10^6$ $lb.in^2$.

This is close to the values found in the benchmark examples of the CLT handbook, which is $EI_{eff} = 440.10^6$ $lb.in^2$. The effective bending stiffness is tested in the APA's Standard for Performance-Rated Cross-Laminated Timber. For this type of layup the bending stiffness is measured to be $EI_{eff} = 475.10^6$ $lb.in^2$.

2. Shell element versus solid element

In order to get the best mechanical accuracy, the element used to model the panels must be chosen with special care. For this type of problem, we could use a 3D solid finite element or a shell finite element. In the shell theory, the membrane and the bending action are taken into account. The horizontal load should generate mostly bending deformation in the plane. Shell theory has been developed for element, where the thickness is significantly smaller than the other dimensions. The shell theory is applicable when the aspect ratio is less than 0.1. Here, for a three layer CLT panel, the aspect ratio is:

$$Slenderness\ ratio = \frac{Thickness\ (t)}{Characterisitc\ Length(l)} = \frac{0.375}{10} = 0.04 < 0.1$$

Shell element is then preferred over solid element for the wall parts. ABAQUS V6 (2011) has two types of shell elements:

- a conventional shell, with 3 translational Degrees Of Freedom (DOF) and 3 rotational DOF, and
- a continuum shell, with only 3 translational DOF.

There are several advantages to use continuum shell element rather than conventional shell element:

- the continuum shell element has less DOF, and the computation time is then reduced. This is particularly interesting for large models, such as the skyscraper model;
- layer-wise composite theory is employed with continuum shell elements. It provides a more refined response for a composite section;
- the continuum shell is also more suitable for contact modeling. Those elements are 3D partially condensed into a 2D shell. The contact between surfaces is then easier to defined and more accurate. Quadratic interpolation cannot be employed with continuum shell elements, but linear interpolation has been preferred here, to reduce the computation time.

The continuum shell element has been chosen for the wall panel and a 3D solid element for the floor panel. For the floors, 3D solid elements have been chosen rather than shell element because of the necessity to have an accurate idea of the forces at the nodes where the isolation systems are connected. It also suits better to simulate the horizontal slip of one diaphragm layer relatively to the other, which is the mechanism that is expected to occur. The long span could add higher modes of vibration with shell, which is must be avoided in diaphragms.

3. CLT definition

The CLT section is defined as a shell composite section. The geometry retained is 3 layers thick for the wall panel and 7 layers thick for the diaphragm panel. In the CLT industry the outside layers are parallel to the gravity loads. So for the walls panels, the two exterior layers are vertical and the middle one is horizontal, as shown below. The layers' relative thickness is one third of the total thickness of the wall panel. A representation of CLT section with ABAQUS V6 (2011) is depicted in Figure 4.

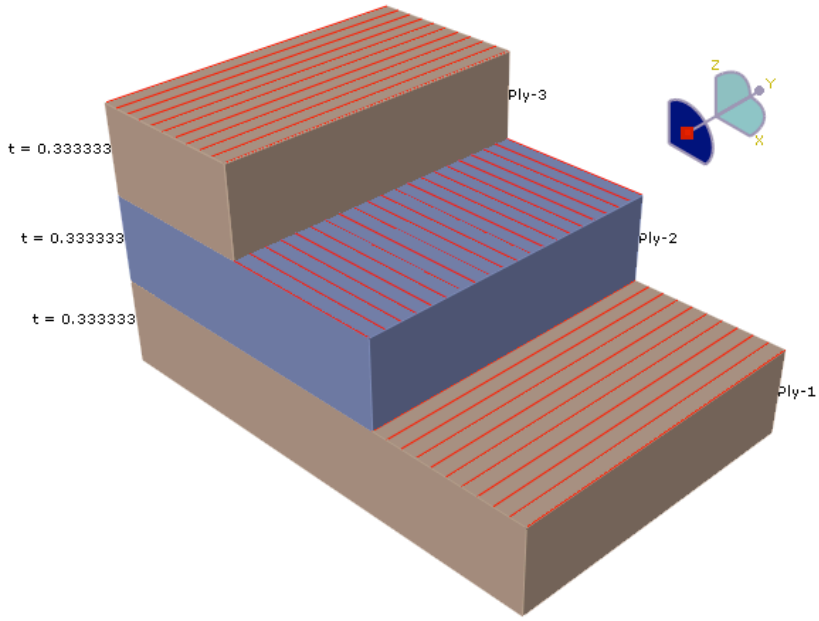

Figure 4: View cut of CLT composite material for wall panel in ABAQUS V6 (2011)

In order to get the cross-sectional behavior of the shell, the section is integrated during the analysis. The Gauss quadrature with two integration points is preferred because it saves computational time with the same level of accuracy.

B. Connectors

Three types of nonlinear connectors are used to anchor the panels or to link them together. The inelastic behaviors are defined in the 3 directions of translation. Each wall panel is connected to the adjacent wall panels with 8 connectors and to the floor panels with 4 connectors. For one story a total of 60 connectors are defined. To simplify the process, the assembled fastener tool available with ABAQUS V6 (2011) is used. This technique is very powerful to duplicate a connector and its constraints to many locations. A template model describing the properties of the connector section and the constraint of the surfaces must be defined. The surfaces that are connected and the position of the connector are then specified in

the fastener definition. The template model is then transposed at each location during the generation of the input file.

1. Panel-to-panel connector

These elements are used to extend the wall panels. This connector idealizes the behavior of interlocked panels by Tongue and groove joints. Dowel-type fasteners distributed over the height are used to completely unify the panels. For simplicity in the model, the fasteners are discretized at four locations over the height. The stiffness in the y-direction and in the positive x-direction is equal to the stiffness of a fastener times the number of fasteners between two discretized locations. The inelastic stiffness of the fastener is taken from: "Inelastic Stiffness Moduli for Nail Joints Between Wood Studs and Plywood Sheathing", by Joseph R. Loferski (1980). The spacing of the fasteners is taken as 12in. on center. In the negative x-direction and in the z-direction, the panels are bearing on the others; it is assumed that the stiffness is considerably higher compared to the y-direction. The stiffness used for the wall-to-wall connector is illustrated in Figure 5.

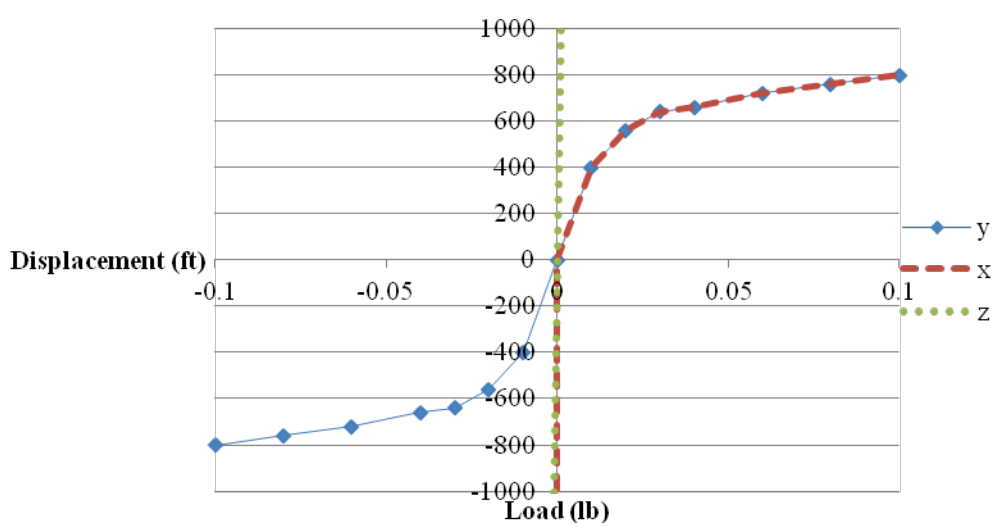

Figure 5: Load-displacement curve for panel-to-panel connector

For this connector, it is shell elements that are in contact. The localization point of the connector must then be tied on the surfaces.

2. Wall-to-panel connector

This connector is an angular metal bracket that links the horizontal panel to the wall panel. The stiffness has been estimated with a finite element analysis of a macro element model. The displacements of a 6 in. by 4 in. by 2 in. parallelepiped solid element with a metal material definition has been measured for different load cases. The distribution of brackets along the base is in accordance with the configuration 2S of the CLT handbook. It is assumed that each panel is connected to the adjacent floor and roof with two brackets at 1/3 and 2/3 of the panel's width. The load – displacement curve is provided in Figure 6 below.

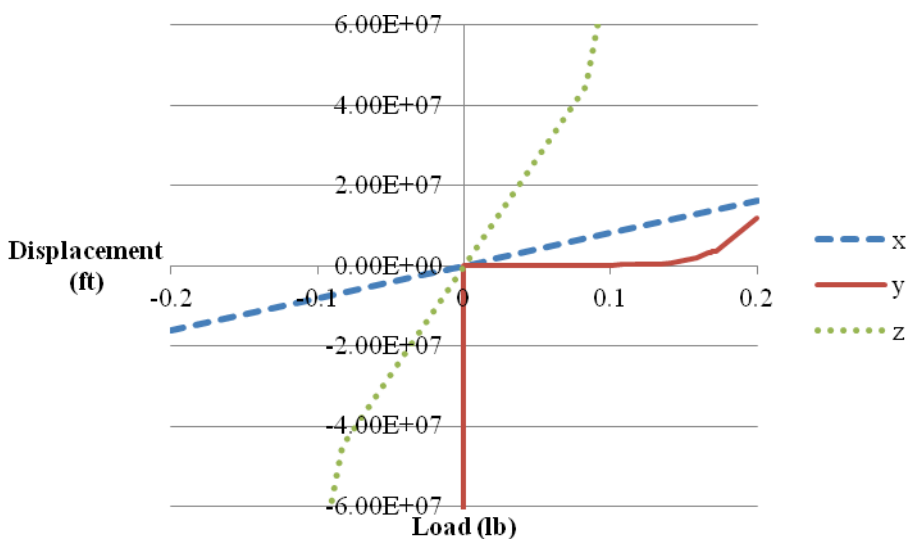

Figure 6: Load–displacement curve for wall-to-panel connector

The behavior is linear in the x-direction only. The wall-to-panel connector prevents the negative vertical displacement, and the uplift is somewhat allowed until a certain distance. The displacement is strongly restricted in the out-of-plane direction. Here the 3D solid elements of the floor are in contact with the shell elements of the wall. The connector and the shell element

have the same number of DOF, but the 3D solid has two times more DOF than the others. The localization points are constrained to the surface of the 3D solid by continuum distribution.

3. Rod connector

The rod connector element is used at each free end of the wall. It is made of a vertical metallic rod that links the bottom of the panel all the way to the top. Metal plates, located at the top and bottom of the panel, prevent the panels from rotating. Displacement is then restricted in the y-direction only. The panel is free to move in the positive direction but is constrained in the negative direction as shown in Figure 7.

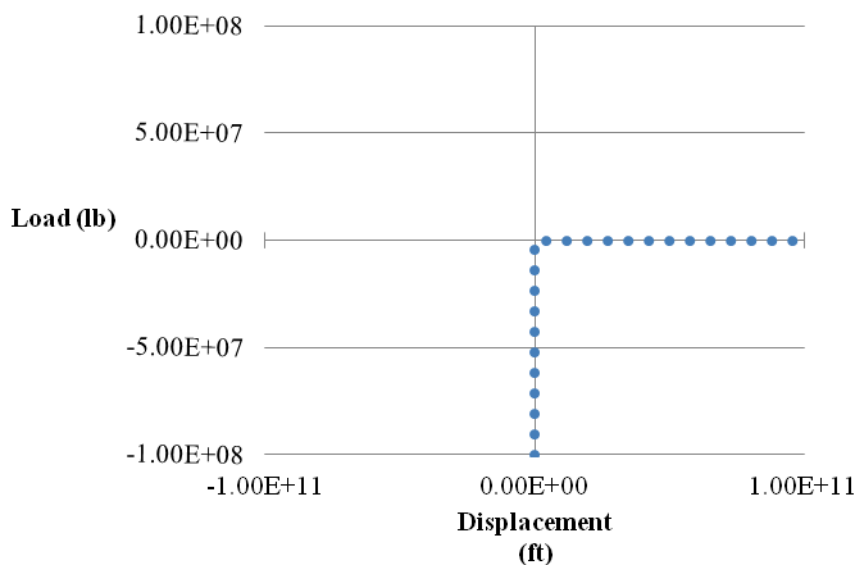

Figure 7: Load-displacement curve in the y-direction for rod connector

IV. Assembled models

In a CLT skyscraper we can anticipate that the deformation will be predominant in the connectors. Connector elements are the unique elements to have an inelastic stiffness definition because they have a much ductile behavior compared to the CLT panels. In seismic design, a positive post-elastic stiffness has a significant influence, compared to an elastic stiffness. A structure with an inelastic stiffness will see its natural period increased and possibly experience a reduced acceleration response. It is then of great importance to adjust the stiffness combination of CLT elements and connector elements. In the model, the only parameter that can be adjusted is the panels' lengths. Smaller panels result in a higher number of connectors, and vice-versa. A model of a 50ft. shear wall has been used to study the influence of the segment aspect ratio and the associated change in the number of connectors on the overall shear wall stiffness and deflection capacity.

A. Shear wall model

The shear wall model was run for different panel segment sizes: 5 ft., 10 ft., 25 ft. and 50ft. The height was held constant and equal to 10 ft. A shear traction was applied on the upper horizontal edge. The magnitude of the shear load ranged from 0 to 125 plf. This is in the range of loads that shear walls usually undergo in small residential or commercial buildings. A general contact element with a high compression stiffness and a low tangential behavior was used to prevent panels from overlapping.

An image of the model for a wall segment width of 5 ft. is displayed in Figure 9. Points at the base represent the bracket connectors; crosses represent the tongue-and-groove joint & screw

connectors. A dynamic implicit analysis was run for each wall segment size, using a edge traction loading as shown in Figure 8.

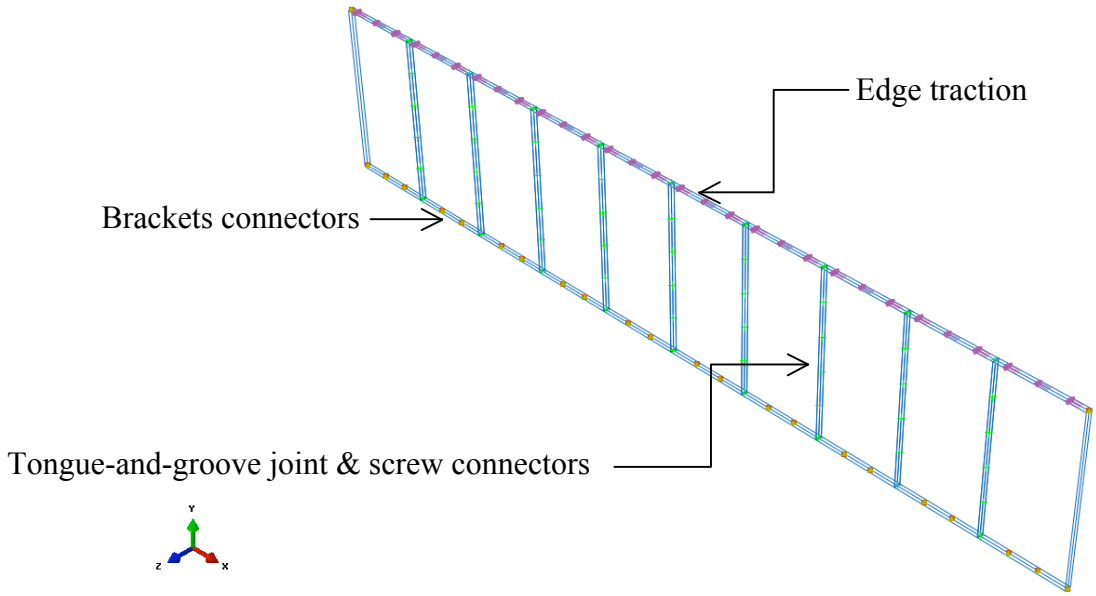

Figure 8: Shear wall model with a wireframe render

B. One-story model

1. Single floor model

A single floor was first modeled. The shear wall model was used to model the four exterior walls. The elements used for the floors were defined with 3D solid elements, with mechanical properties representing a 7-layers CLT section. A trench has been modeled all around the diaphragm perimeter. The trench is designed to leave a space between two adjacent floor layers in order to position the distributed base isolation elements (i.e., viscous dampers and re-centering springs). The trench is 0.250 ft. deep and 5 ft. wide and is illustrated in Figure 9. The dampers and springs will experience a considerable amount of force. In the real world, the springs and dashpots could not be directly attached to the CLT panel. A metal plate should link spring and CLT together. A metal property definition was assigned to the elements in the trench

to model this plate action and distribute the connection force over a larger area than a single point.

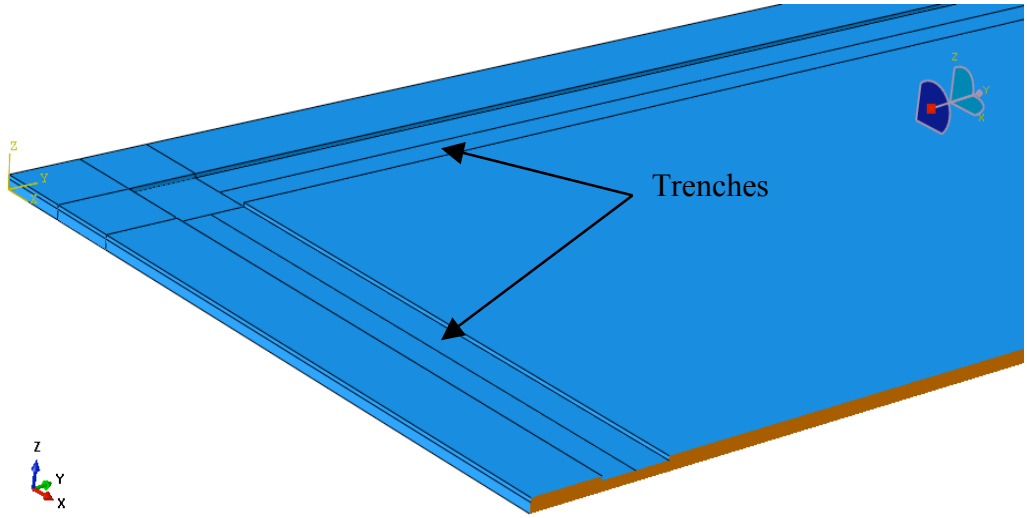

Figure 9: View cut of the diaphragm part

A section of the single story model is depicted in Figure 10. The top floor portion has been removed to show the interior walls. The different points are the locations of the different connectors.

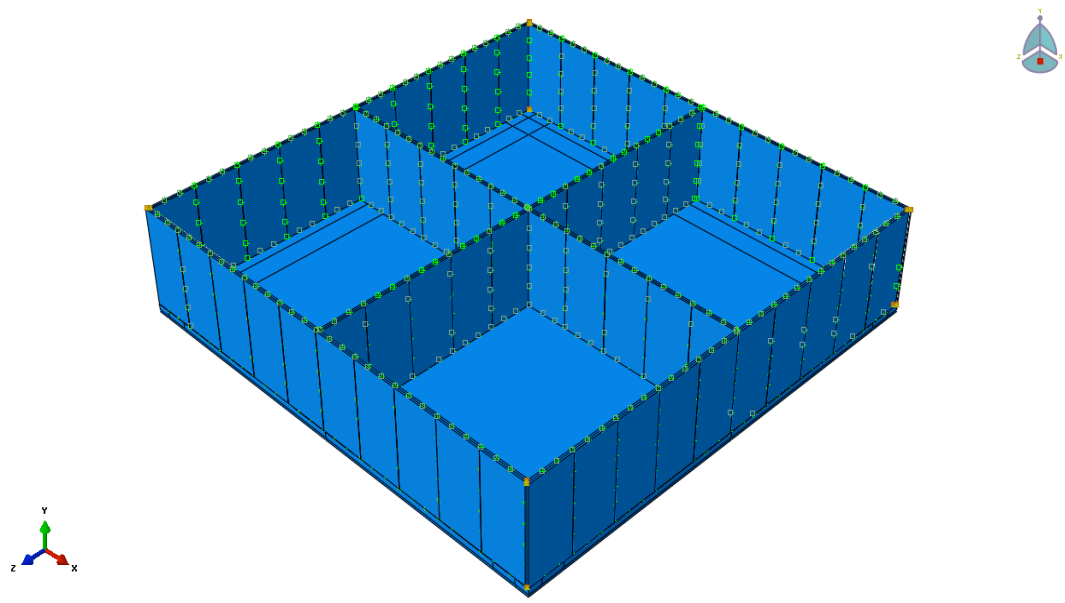

Figure 10: Bottom section of the single story model

2. Substructure generation and skyscraper assembly

A substructure technique was used to reduce the computation time and facilitate the assembly of the skyscraper model. It assumes that the substructure will experience small deformations only. In ABAQUS V6 (2011), a substructure is the output result of a substructure generation step. The theory of substructure generation is to condense the stiffness of eliminated nodes to a small number of retained nodes. The stiffness, the mass and the damping matrices of the eliminated nodes is calculated and applied to the retained nodes. This process is extremely useful when identical parts appear several times in a model, such as a story here. The process used to generate the substructure is described below.

a) Contact interaction generation

A static step is run first. This step is used to compute the contact interactions between the different surfaces. A stiff compression behavior and a soft tangential behavior are used for all the contact connector properties. These interactions will prevent the elements from overlapping

during the analysis. During this step, the forces applied must self-equilibrate in order to reach the equilibrium at the end of the step. The interference fit between surfaces in contact is the usual technique to apply self-equilibrating forces to a structure. The interactions were tested with gravity loading.

b) Substructure generation

A frequency step is run before generating the substructure. This step allows ABAQUS V6 (2011) to extract the Eigen modes of the single-story model. The first 3 modes are extracted, which is usually sufficient for most structures in the civil engineering world. This extraction increases the computational cost, but it has to be completed only one time and can be used multiple times during the analysis of the full structure. Dynamic modes are added to the static modes during the substructure generation to improve the dynamic representation. The stiffness, mass and damping matrixes are reduced and the non-retained elements are eliminated. To properly assemble the substructures together and to increase the precision, a total of 34 nodes per story were retained.

C. Skyscraper model

The substructure part, representing a story, was imported in a new model with multiple substructures to represent a high-rise building. The benefit of having one story defined as a part is that it can be repeated in the assembly module. An instance of a part can be added, deleted and moved very easily. Any number of stories can then be achieved but this analysis is limited to 10 stories. The 10 substructure modules are connected to the adjacent ones by the retained nodes.

If the story is isolated, the substructure modules were connected with the spring and dashpot elements. For linear analysis, ABAQUS V6 (2011) allows models springs and/or

dashpots to be modeled between two nodes by setting a spring stiffness and/or a dashpot damping coefficient. It is assumed that the mass of the isolators is negligible compares to the mass of the story, so no associated mass is added. The non-isolated stories are tied directly to the adjacent floors. A link with a tie connection type is used. Using a linear Multi-Point Connector (MPC) such as a tie connector in an implicit dynamic analysis allows both the displacement and the velocity to be constrained exactly.

1. **Gravity loading analysis**

Before applying the seismic loading, the structure is assumed to be at rest, resisting only its self-weight. This first period is modeled with a general static step. A gravity load is applied to all the substructures and roller boundary conditions are applied to the bottom nodes of the first substructure.

2. **Earthquake loading analysis**

A time-history analysis was preferred because it provides the possibility to estimate time-dependent earthquake traces. Any earthquake event available in the Pacific Earthquake Engineering Research center (PEER) archive is then easily used as the input excitation. This choice eliminates the use of frequency analysis. A direct integration solver has been preferred over modal dynamic methods (such as transient modal dynamic with ABAQUS V6-12), because a dynamic modal analysis requires the extraction of the vibration modes first. A frequency-extraction step must then be run which reduces the cost effectiveness of the modal dynamic analysis. Another argument for the direct integration was the possibility to implement various sources of damping. Indeed the choice of viscous dampers for the isolation system has been made at the beginning, but friction dampers could be more practical in a real application. The

need to compare two alternative system configurations was then necessary, which can only be accomplished with direct integration methods.

Finally the implicit scheme has been chosen over the explicit scheme for its constant time increment and its numerical stability. The fact that the implicit method is widely used in the civil engineering world was also an important argument for the author. The analysis time increment has to be equal to the period of time at which the acceleration values are given in the earthquake trace, which is usually 0.02 seconds.

During an earthquake, the ground acceleration shakes the structure through the foundation. The seismic load for the numerical analysis is simulated by applying an acceleration at the lower nodes of the model. In ABAQUS V6 (2011) you can define an acceleration with a magnitude in each direction and an amplitude curve. The magnitude in each direction was set to $g = 32.2\ ft/s^2$. The amplitude curves of historical earthquake event were extracted from the PEER Ground Motion Database. During this research, several earthquakes have been used. The normal to fault acceleration was applied along the 1-direction, the orthogonal to fault acceleration was applied along the 3-direction and the vertical acceleration was applied along the 2-direction.

V. Results discussion

A. Models validation

1. Elements' stiffness

a) Panel

Patch tests have been performed to check that the stiffness of the elements was correctly defined. The accuracy of the wood definition has been measured by a tensile test along the 3 directions. A solid part with a homogeneous section has been used. The three first diagonal parameters of the stiffness matrix [D] have been calculated by dividing the normal stress with the normal strain given as outputs. The results of these analyses are given in Table 3. Considering the approximation and the rounding errors, the error between inputs and outputs seems reasonable.

Table 3: Results of tensile tests in 3 directions

	Actual (psf)	Model result (psf)	Relative error
D_{1111}	14,710,863.3	14,638,716.5	0.5%
D_{2222}	8,457,233.7	8,437,500.0	0.2%
D_{3333}	301,333,063.8	299,093,655.6	0.7%

b) Connectors

The connectors have been tested in a same manner; Figure 11 gives the output of a tensile test of a wall-to-wall connector. The dashed line represents the model prediction and the solid line represents the experimental results from nail tests conducted by Loferski (1980). As can be

seen in Figure 11, the outputs given by ABAQUS V6 (2011) match almost exactly the inputs described earlier.

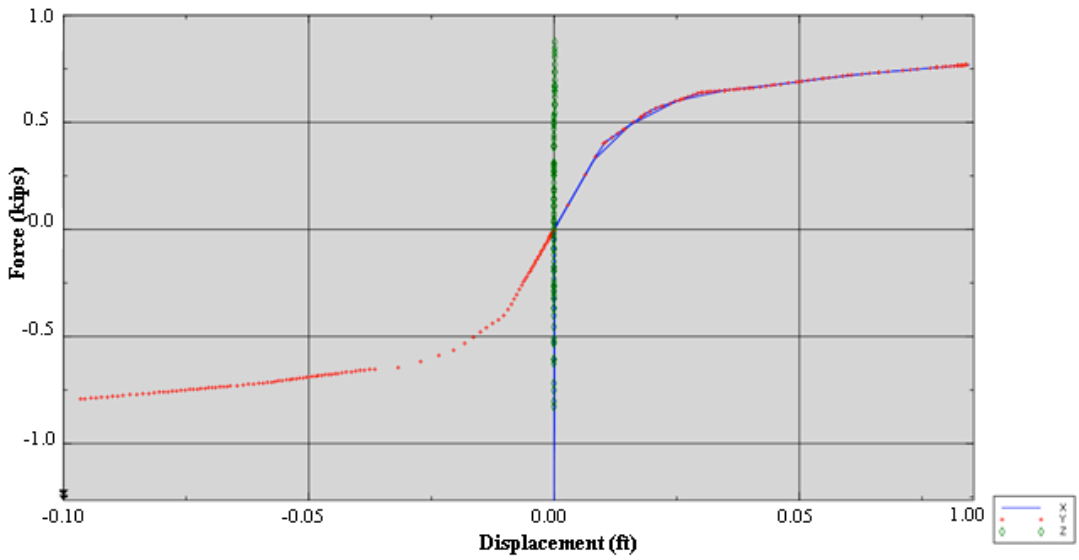

Figure 11: Outputs of finger joint & screw connector tensile test

2. CLT section

The cross-sectional stress distribution has been studied to validate the composite model. A patch test for different loading configurations has been performed. Plots of the normal and shear stresses through the thickness are illustrated in Figure 12.

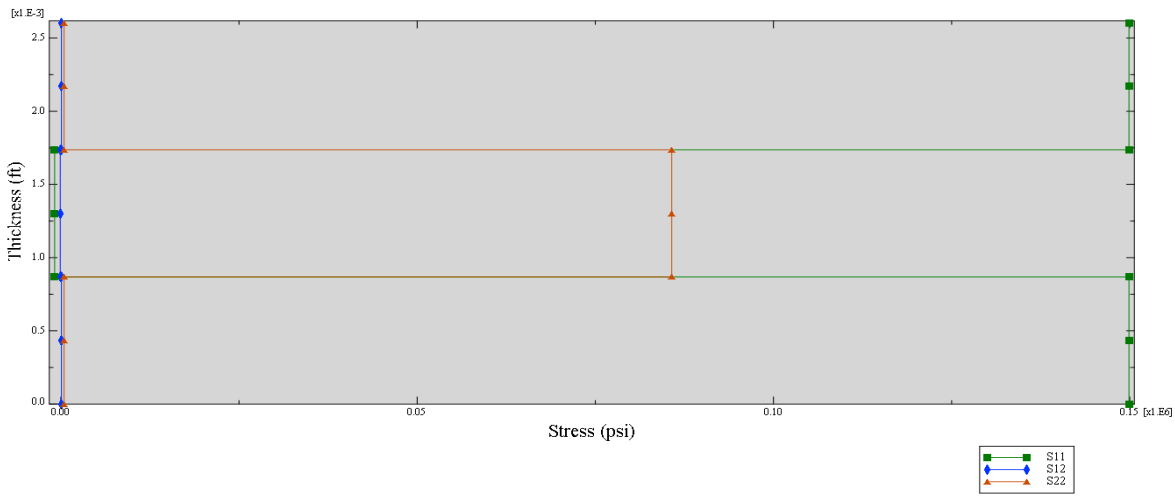

Figure 12: Outputs for tension applied in the 2-direction

In Figure 12, the normal stress along the 2-direction (S22) is higher in the middle layer than in the exterior layers. In order to satisfy the continuity condition, the strain must be constant through the thickness (no unevenness along the section). As $\varepsilon_2 = E_2 . \sigma_2$, the stiffness has to be higher in the 2-direction for the outside layers than in the middle layer ($E_L > E_R$). This is in agreement with the expectations. From Figure 12, the normal stress along the 1-direction (S11) is higher in the exterior layers than in the middle layer. As, $\varepsilon_1 = -\nu_{12}.\sigma_2/E_2$, the Poisson's ratio has then to be higher in the middle layer than in the exterior layers ($\nu_{RL} > \nu_{LR}$).

A tensile test has been performed for each direction. The results meet the expectations, and are presented in Appendix A.

3. One-story model

The one-story model was submitted to a gravity loading to check that the connectors and the mechanical properties are properly defined. The resulting vertical displacement is depicted in Figure 13. According simple static calculations, the interior walls' tributary area is double the tributary area of the exterior walls. The deflection of the interior wall should be twice the

deflection of the exterior wall. The ratio given by ABAQUS V6 (2011) is: 2.8. The difference can be explained by the metal plate definition used in the trench around the perimeter of the diaphragm. The metal plate stiffens the section close to the trench, which results in a lower deflection at the exterior walls.

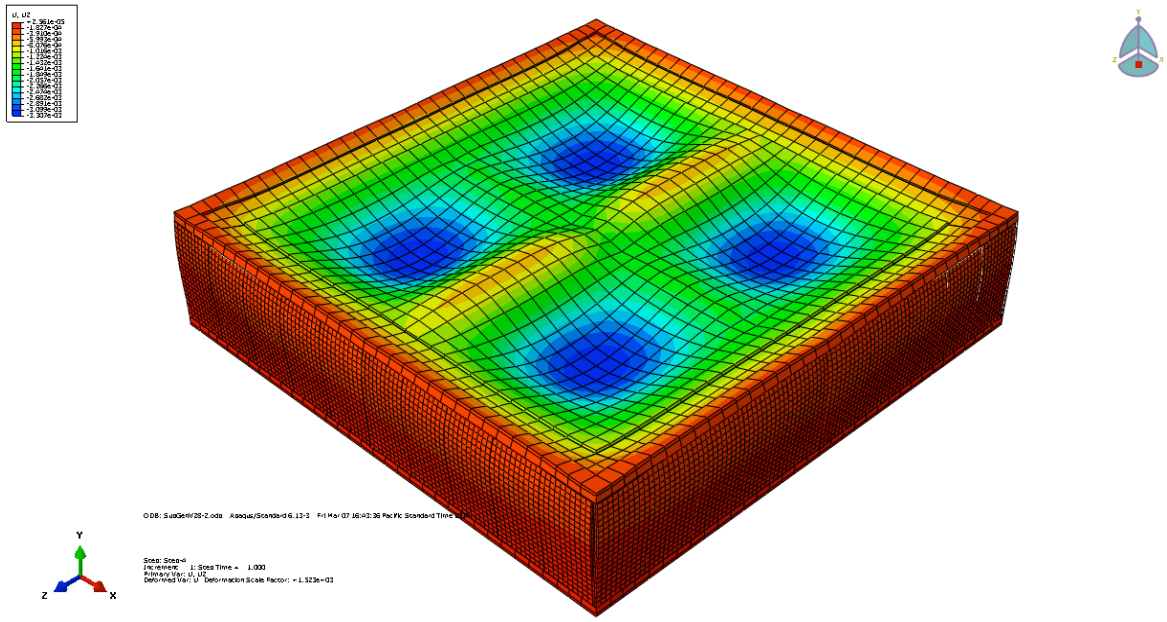

Figure 13: One-story model under gravity model (deformation factor: 1,523.2)

4. Dynamic behavior

A two-story model was been used to validate the dynamic behavior of the substructure assembly. Two substructures are connected together with springs. A constant acceleration of 1 ft/s^2 is applied in the horizontal direction. The equation of motion for this condition is:

$$kx + c\dot{x} = m\ddot{x}$$

where, *m* is the mass of one story, *k* the total spring stiffness, and c the total damping coefficient. The solution of the differential equation of the undamped system is:

$$x(t) = -\frac{1}{\omega_0^2}\left[\cos(\omega_0 t)e^{-\delta t} - 1\right]$$

where, $\omega_0 = (k/m)^{0.5}$ the natural frequency and $\delta = c/(2m)$ the damping ratio. The closed-form solution and the model output displacements are plotted in Figure 14. The amplitude and the frequency match quiet well, the averaged relative error is below 20%. The difference is due to the assumptions made in estimating the stiffness and the damping of the structure. They have been assumed to be equivalent to the stiffness and the damping coefficient of the isolators in parallel to the stiffness and damping coefficient of the story box.

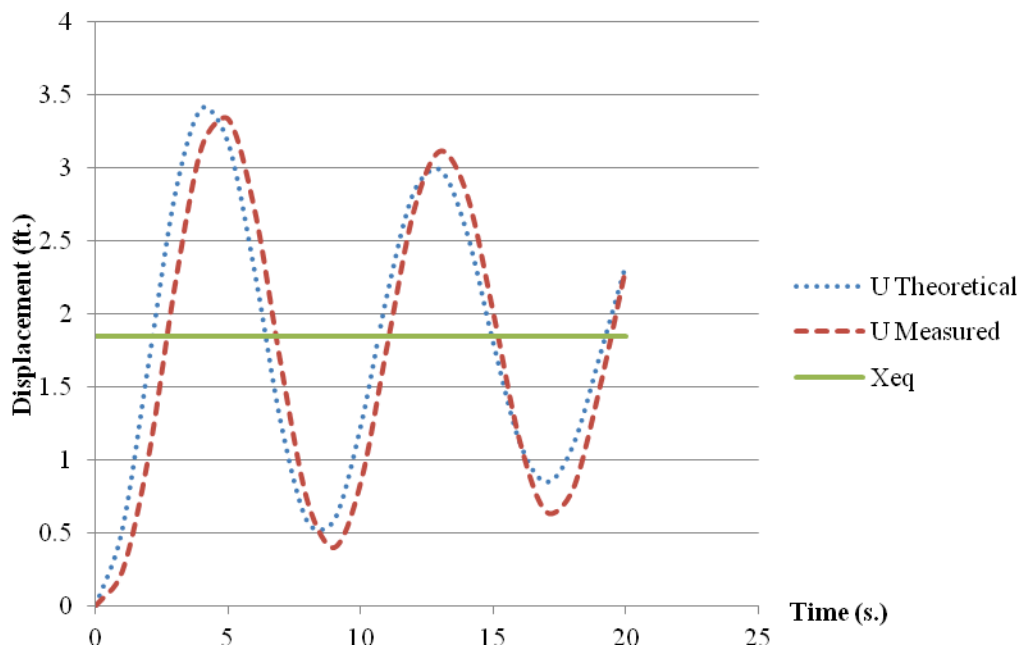

Figure 14: Dynamic test of two stories isolated

B. Influence of panel's ratio

An important unknown is how the panel width influences the total deformation. In seismic design, a ductile behavior can lower demands on the structure. It is then beneficial to let the building drift up to a certain value, below the failure point. The American Society of Civil

Engineers (ASCE) limits the story drift to between 0.01 and 0.02 times the story height below the story level, depending on the building occupancy category (ASCE 7-10, table 12.12-1). Here, if a building of 10 stories is assumed, the total height would be 100 ft, the maximum horizontal deflection allowed would then be 2 ft.

The results of the 50ft shear wall model are used to choose the best panels' aspect ratio. The force displacement curve for different wall panel segment is given in Figure 15.

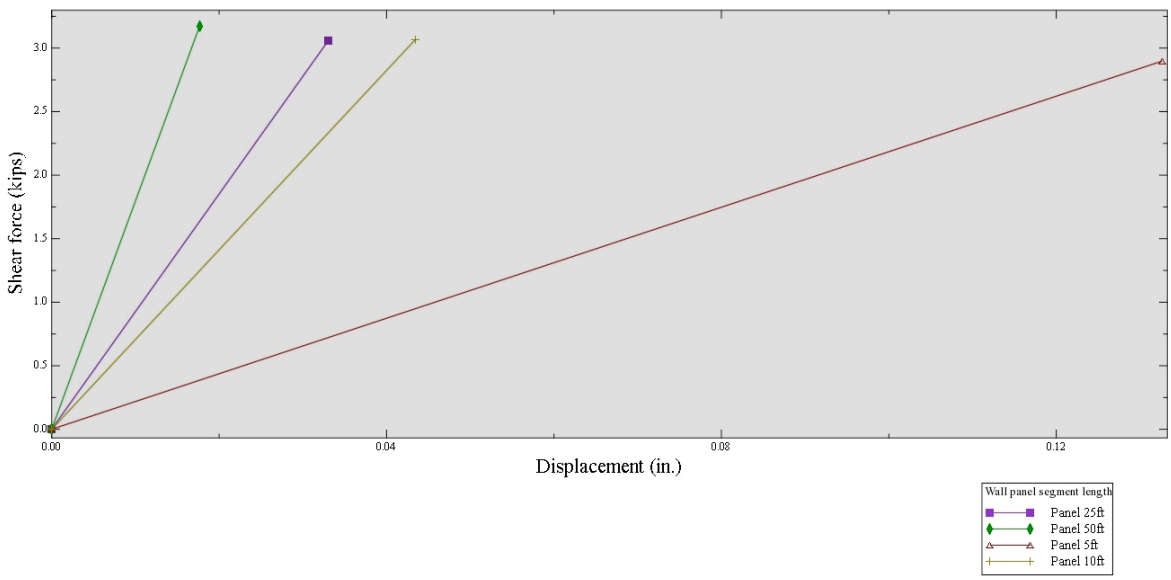

Figure 15: Stiffness vs. aspect ratio of shear wall models

Because: $T = 2\pi/\omega$, and $\omega = (k/m)^{0.5}$ (where ω is the natural frequency of Mode 1, T the natural period of Mode 1, k the stiffness and m the mass), lower stiffness means higher natural period and a possible reduced acceleration response. The panel segment length is related to the number of wall-to-wall connectors. Table 4 gives the stiffness of the 50ft shear wall model for different number of wall-to-wall connectors. Shear wall with 5ft. panels segment length has the lowest stiffness.

Table 4: Number of wall-to-wall connectors and overall wall stiffness for different wall panel segment length

Panel size	Numbers of wall-to-wall connectors	Wall stiffness (kips/in)
5 ft.	54	1.7
10 ft.	24	5.7
25 ft.	6	7.8
50 ft.	0	15.7

If it is assumed that each floor deforms the same amount, the maximum drift of a 100 ft. building would be 0.14 x 10 = 1.4 ft. if the walls use 5 ft. long wall segments. This is in the range allowed by the ASCE. A segment length of 5 ft. was then been chosen as the "best" size for the wall segments for the one-story model.

It is also important to consider the displacement capacity of the shear wall design. The displacement capacity is inversely proportional to the aspect ratio. Smaller aspect ratio means higher displacement capacity. This is understandable because the rotation of each panel is more important for wider panel. This positively satisfies the choice made above. The fracture is not taken into account in the model, but it is possible to estimate the minimum load at which a failure of the connectors can be expected. The shear wall model with a 5ft. wall panel length has been run with an increasing traction load on the upper edge. The maximum deformation capacity of a metal fastener is around 1.5 in. This maximum displacement has been reached at the bottom of the end panel wall for a surface traction of 675 plf approximately, as shown in Figure 16. For this load, the horizontal displacement of the top part of the panels is 5.4 in. In the same situation, with the 10 ft. long panel wall, the horizontal displacement at the upper edge is 3 in. The horizontal displacement capacity of the wall is then smaller when using wider panel segment.

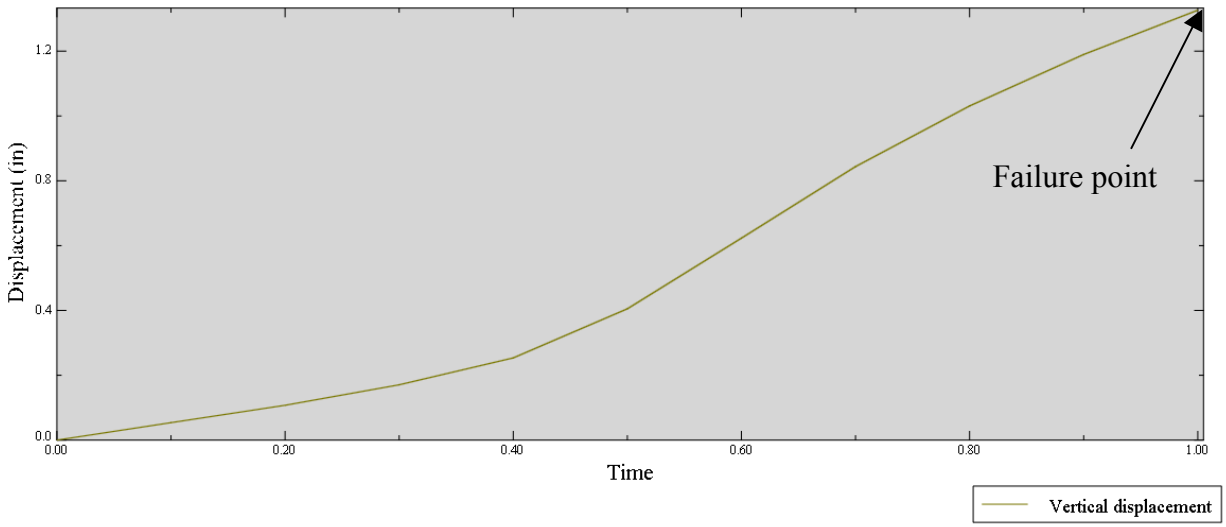

Figure 16: Vertical displacement over time at the lower edge of the shear wall model with 5 ft. panel length

The influence of the stiffness definition of the connectors has also been investigated. The stiffness of the wall-to-wall connectors has been multiplied by 2 and 5. The multiplication by two corresponds to a initial screw spacing being divided by two and the multiplication by 5 reproduces the use of glue instead of screws. From Figure 17, when increasing by 50% (multiplied by 2) the wall-to-wall connectors' stiffness, the overall shear wall stiffness is increased by 18%. When increasing by 150% (multiplied by 5), the overall stiffness is increased by 45%. The wall-to-wall connectors play a significant role in the shear wall response but a small variation (below 25%) around the initial stiffness can have an impact on the response that can be neglected.

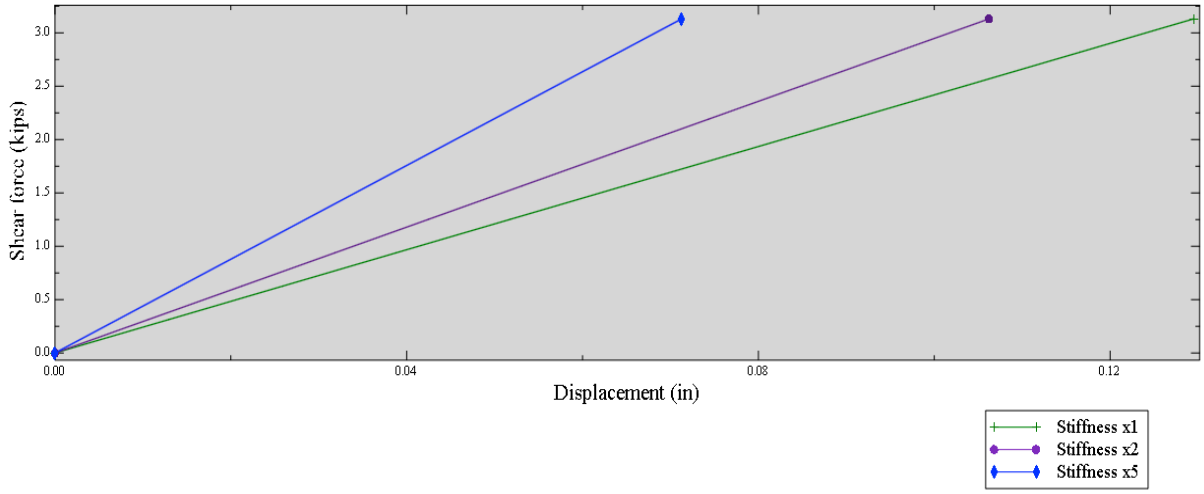

Figure 17: Stiffness vs. wall-to-wall connectors definition

C. Skyscraper analysis

1. Base isolation parameters

Each isolation configuration is named by the highest level being isolated. For example Isolation 3 refers to a structure with the first three stories being isolated. Isolation 1, 2 and 3 are depicted in Figure 18.

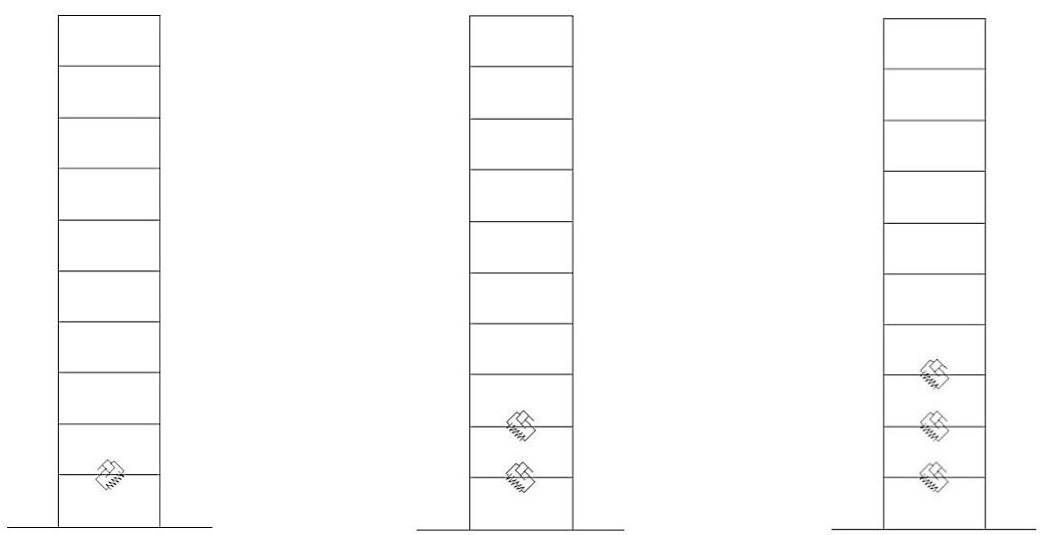

Figure 18: Configuration of isolation 1 to 3 (left to right)

a) Spring stiffness determination

To be rational, the displacement along the slip plane of the isolated stories must be limited to a realistic value. To keep the utility connections simple, a maximum displacement of ½ foot at any level was chosen. With that maximum slip displacement, an Isolation 5 configuration would have a total slip displacement of 2.5 ft, which remains below the 3ft. displacement of traditional base isolated structure. The stiffness of the springs was adjusted by trial and error to meet that limit. The stiffness necessary to allow up to ½ ft. slip for configurations with the first through fifth floors isolated are presented in Figure 19. From Figure 19, it appears that isolating more than three stories has a negligible effect on the response of the upper stories. There is no stiffness required to limit the slip displacement to ½ ft. at stories 4 and 5. Based on these results, it was decided to focus the analysis on Isolations 1, 2 and 3 only.

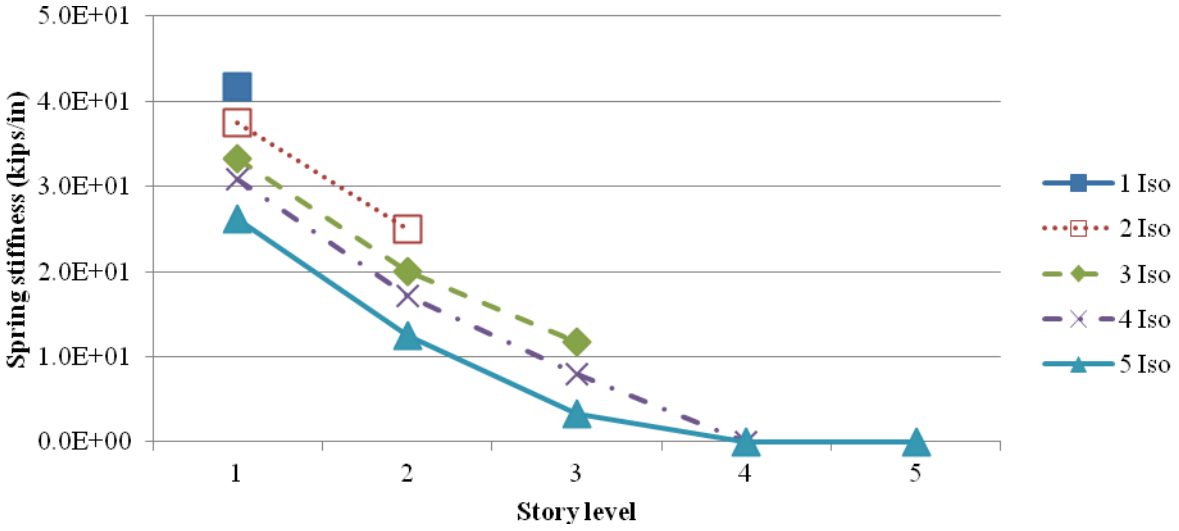

Figure 19: Springs stiffness for a slip displacement of ½ ft.

With the spring stiffness and the maximum displacement, it is possible to estimate the maximum load in the springs. Between Isolation 1 and Isolation 3, there is a reduction of 20% of the demand on the spring. This reduction could be appealing when designing the system.

Isolation 1 is equivalent to a traditional base isolation system, where all the demand is concentrated on the foundation (here the first story). Isolation 2 and 3 highlight the interest of distributed isolation, where the demand is shared on several levels.

b) Damping coefficient determination

In civil engineering, the damping of a structure is usually express as a fraction of the critical damping. A critically damped structure will return to its resting position without oscillating. The critical damping can be calculated with the following equation:

$$\zeta = \frac{c}{4m\pi f_0}$$

The result is the damping ratio (= 1 for critical damping); c is the damping coefficient; m is the mass of the system, and f_0 the natural frequency of the undamped system. The natural frequency can be determined with ABAQUS V6 (2011). The natural frequency is assumed to be close to the frequency of the first mode of vibration. It is possible to make that assumption because the first mode is predominant in the deformation pattern. Frequency analyses were run without dampers, and the natural frequencies are given in Table 5:

Table 5: Natural frequency of isolated and non-isolated CLT skyscrapers

	f_0 (Hz)
Non-isolated	1.218
Isolation 1	0.787
Isolation 2	0.554
Isolation 3	0.422

To visualize how the damping influences on the overall response of the structure, a quick analysis was run. Only a range of 4 seconds around the Peak Ground Acceleration (PGA) of the record was used and the outputs were requested every 0.2 seconds. The results of these analyses

are shown in Figure 20. In Figure 20, there is a reduction of about 75% for the displacement between the un-damped and the critically damped system. The model with 100% critical damping does not behave perfectly like a critically damped system, but accounting for the assumptions the result is close enough and then the method used to estimate the critical damping is reliable. The energy dissipation seems effective from 25% of critical damping, and 50% has a considerable influence on the dynamic response. The proportional increase of the damping coefficient does not result in a proportional decrease of displacement. By increasing the damping coefficient from 0% to 25% of critical damping, the displacement is reduced by almost 55%. The remaining 45% of displacement reduction occurs for a damping coefficient in the range of 25% to 100% of critical damping. The biggest drop in displacement occurs when the damping coefficient is approximately 25% of the critical damping.

In terms of nodal forces at the connecting nodes, a higher damping coefficient would require higher strength in the dampers, which is less cost effective. The nodal forces where one of the dashpots is connected to the CLT floor element were calculated during the analysis of Isolation 2 and are illustrated in Figure 21. From Figure 21, the demand on the connection to the CLT floor is almost multiplied by two when the dashpot damping coefficient was increased from 25 to 50% of critical damping. Based on these results, a damping coefficient of 25% of the critical damping was chosen as an appropriate balance between strength of the damper and displacement reduction.

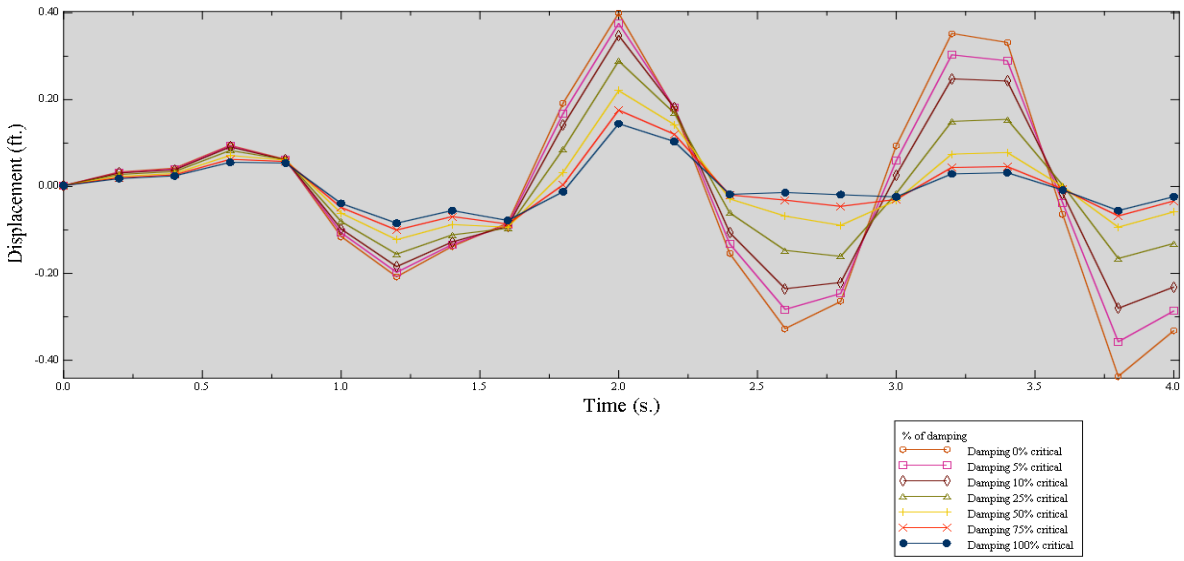

Figure 20: Slip displacements for Isolation 1 for different damping coefficients

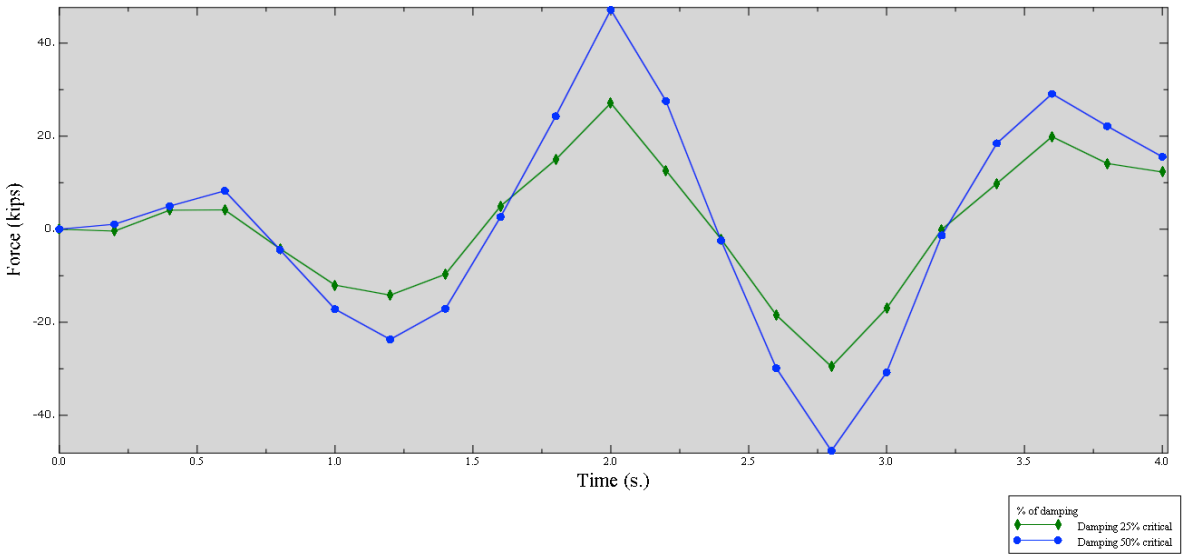

Figure 21: Nodal forces at attaching node on upper floor of story one for different damping coefficients

Structures change with time; the effects of environment and age affect the inner properties of the materials. For example, shrinkage and swelling of wood soften the material. These evolutions are usually characterized by a lengthening of the natural period and an increase

of damping. The increase is usually small, less than 20%, and the effects can be neglected. Here, the isolators' parameters do not account for the fatigue of the building.

2. Canoga park full scale analysis

For the first full-scale analysis, the 20 first seconds of the 1994 Canoga Park were used as acceleration inputs. The earthquake trace used is shown in Figure 22. The PGA is 0.4g at 8.7s. The acceleration spectra is given in Appendix B, the spectral acceleration is maximum at a period below 1s., which is close to the natural frequency of the non-isolated model.

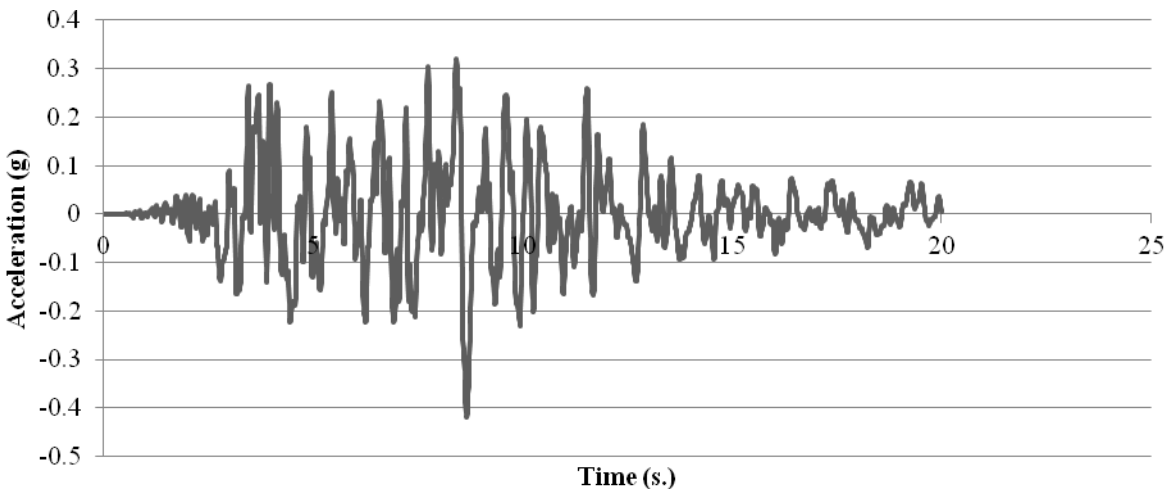

Figure 22: 1994 Canoga Park earthquake trace

a) Non-isolated model

The total displacement of the building is shown in Figure 23. The maximum displacement is 0.646 ft. and which is reached at 13.1 s. As predicted with the frequency analysis, the natural period of the structure is close to 0.8s. For comparison, a 10-story CLT building with a concrete core had a top maximum displacement of 0.5 ft. due to a wind load pressure of 58.5 psf (Van De Kuilen, Ceccotti, Xia, & He, 2011).

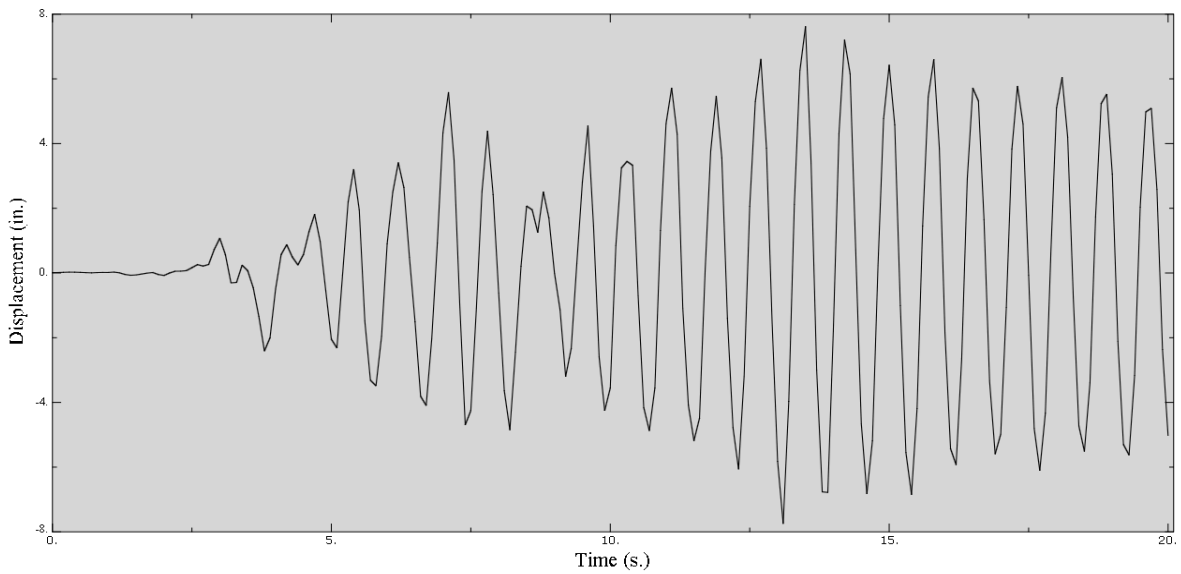

Figure 23: Drift of non-isolated model under 20s. Canoga Park earthquake

b) Isolated model

The springs' stiffness and the damper coefficients presented in section IV - C - 2 were used for the different configurations. For Isolation 2 & 3, the damping coefficient at level *n* is proportional to the mass above the isolated level *n*. The isolators' parameters used for the full scale analysis are presented in Table 6.

Table 6: Springs stiffness and dashpots coefficient for full scale analysis

		Story level		
		1	2	3
Configuation 1	Spring Stiffness (kips/ft.)	500		
	Damping Coefficient (slug/s.)	28,000		
Configuation 2	Spring Stiffness (kips/ft.)	450	300	
	Damping Coefficient (slug/s.)	3,000	18,000	
Configuation 3	Spring Stiffness (kips/ft.)	400	240	140
	Damping Coefficient (slug/s.)	1,700	1,700	12,000

The displacements for Isolation 1, 2 & 3 are plotted in Appendix C, Appendix D, and Appendix E. The addition of damping reduces the story velocities and accelerations (see Appendix F). The unsecured contents inside the building would then be less impacted.

At the maximum displacement, the story displacements are compared for each configuration in Figure 24. There is a noticeable difference between the isolated and the non-isolated models. For the isolated models, the displacements above the last isolated level are almost constants along the height. This means that the demands on those levels are close to zero. For Isolation 1, the reduction is so significant that the total displacement is less than the non-isolated configuration. By isolating the first story, it is possible to get both the total drift and the panel deformation lowered. Isolation 1 here is equivalent to inter-story isolation case (b) in the analysis by Ryan & Earl (2010). In this study, a slip displacement of 0.9 ft. was estimated for a PGA of 1.5g of the model for Isolation 1 results in a slip displacement of 0.23 ft. for a PGA of 0.4g. Using a proportional adjustment, the slip displacement would then be 0.87 ft. for 1.5g PGA. This is comparable to the value found by Ryan & Earl. For each configuration, the slip displacement at each level is less than 1/2ft. has expected, and the required utility connections could be configured to be less costly than the high displacement capable connections required for traditional base isolation applications.

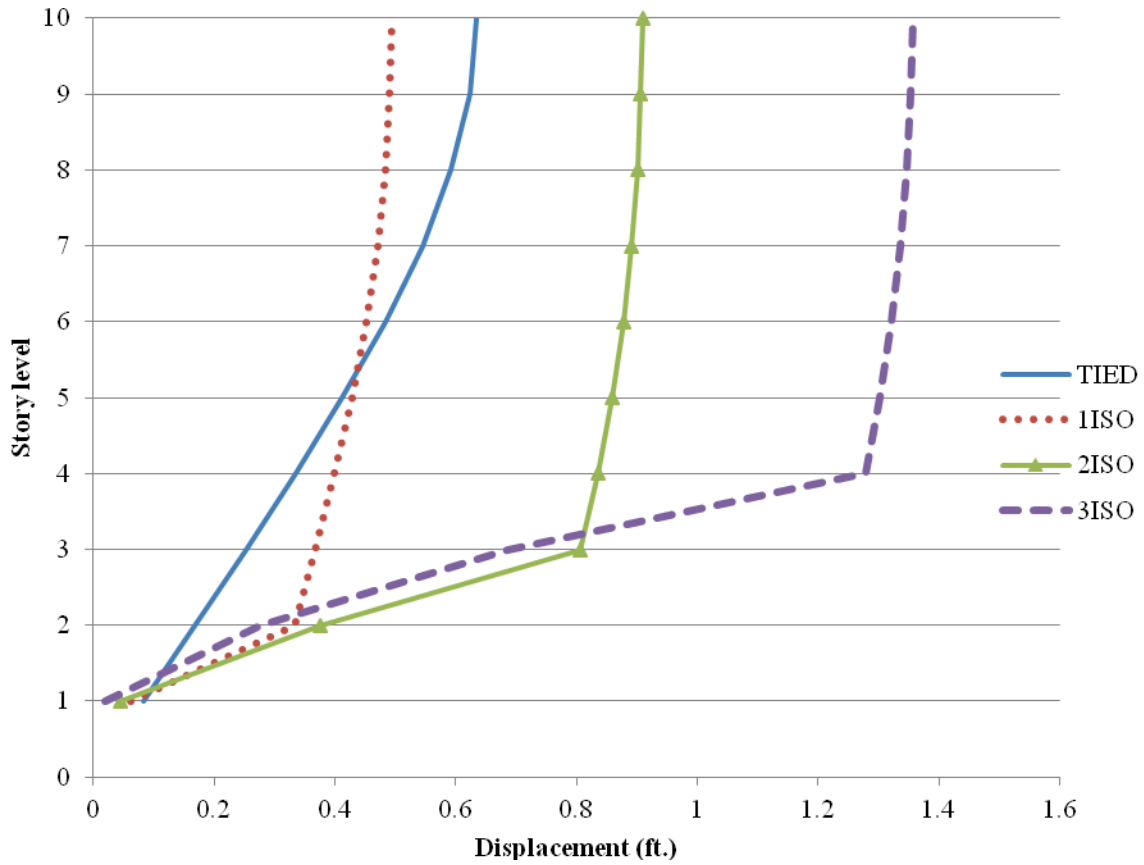

Figure 24: Stories displacement at maximum displacement

From Figure 25, the demand on the shear walls can be compared for different configurations at any story. The graph on the left gives the deformation of the wall in unit of length. The graph on the right shows the shear stress in the wall panels below the slip plane. There is a maximum shear stress at the first level of the non-isolated model of 268 psi. The Standard for Performance-Rated Cross-Laminated Timber published by APA gives a characteristic shear strength (f_v) of: f_v = 425 psi in any layer. The CLT panels should not reach their failure point during this event and remain in the elastic range. The panel deformation is significantly reduced between isolated and non-isolated models. There is an averaged reduction of 65% between the Isolation 1 and the non-isolated configuration. The difference between the

different isolated models is small. The reduction of deformation demand is reduced by approximately 20% between Isolation 1 and Isolation 3. The activation of higher levels does not reduce the wall panels' deformation significantly.

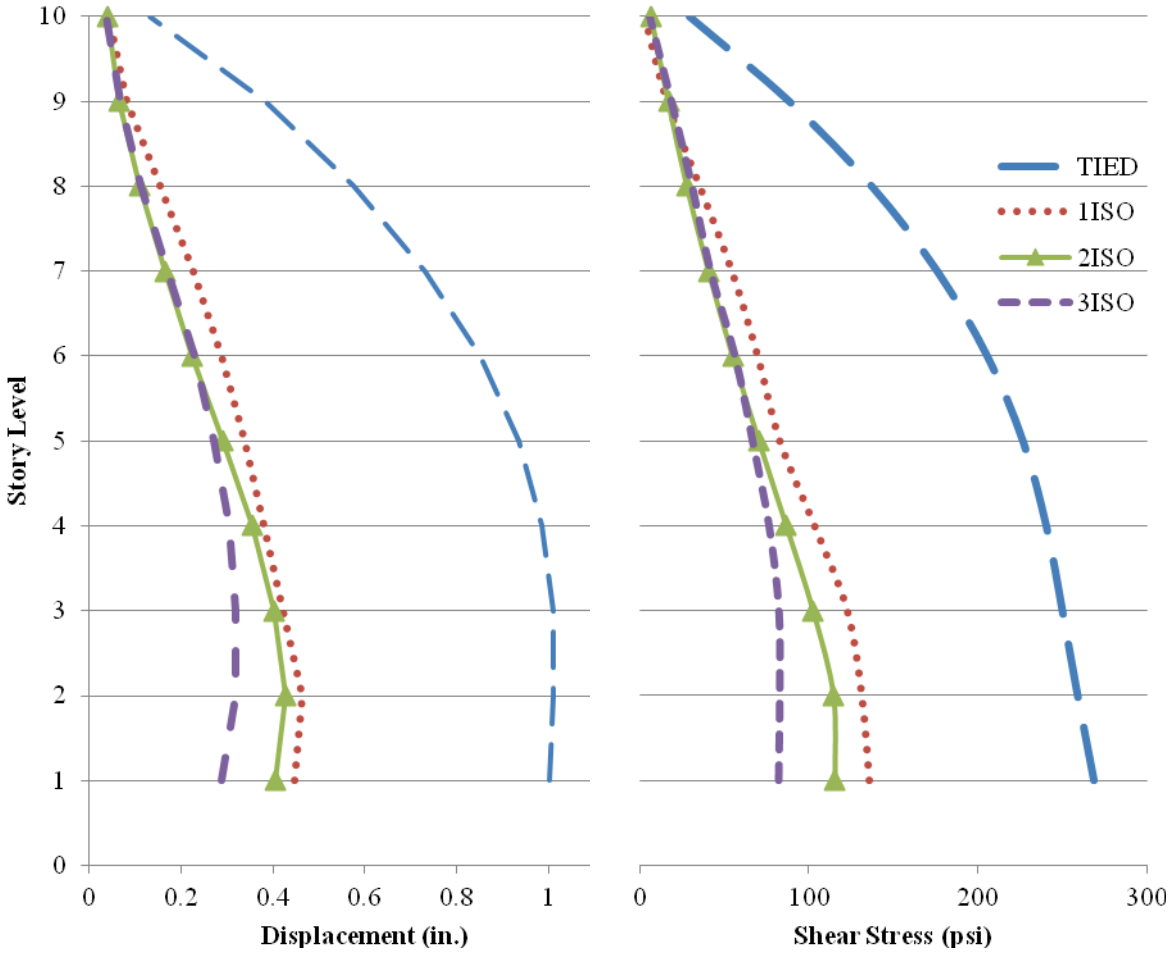

Figure 25: Panels deformation for non-isolated configuration and isolated configuration 1, 2 & 3 at maximum building displacement

The demands on the isolators are plotted in Figure 26. The graph on the left gives the slip displacement at each isolated level; the total force in the springs is proportional to the displacement. The graph on the right shows the force that is required to attach a single damper to the CLT floor. For Isolation 1 the strength of the connection must be at least 28 kips to safely

attach the damper to the panel. The design of these connections might be complex in a real application. It might even be necessary to have more than 2 dampers at each level; to distribute the 28 kips to several nodes.

However, adding more levels of isolation also reduces the force in the dampers. The reduction between each configuration at each level is almost constant and equal to 24%. The damping coefficient of Isolation 3 could be reduced at level 2 to get a more linear distribution. A cost analysis would be necessary to estimate the total gain due to the strength reduction on the isolation system and the floors.

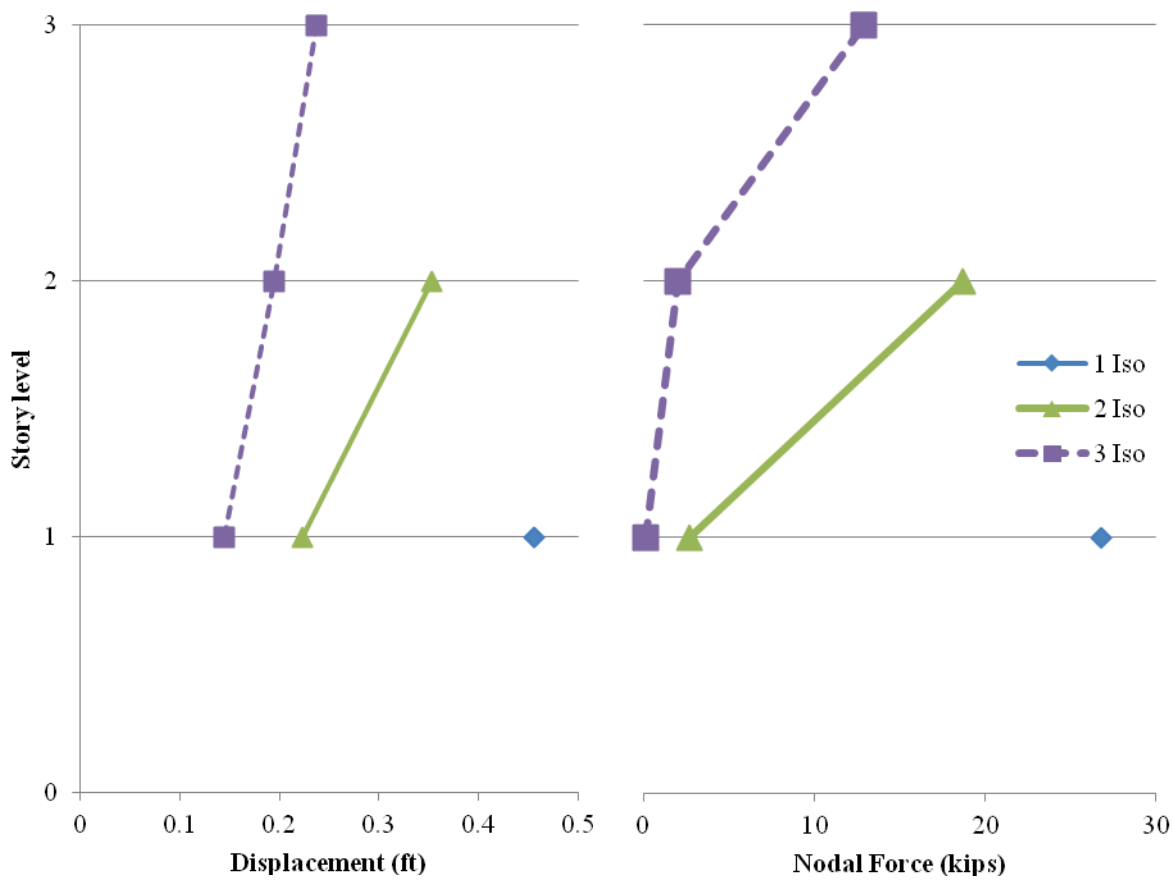

Figure 26: Slip displacement and nodal forces at dampers' connection at isolated levels

3. Kobe full scale analysis

The first full-scale analysis with the Canoga Park earthquake record showed a great improvement when isolating one story or more. The natural period of this earthquake was close to the natural period of the non-isolated structures. It is expected for the isolation systems to be less effective for an earthquake with a longer natural period. The 1995 Kobe, Japan earthquake was used for the second full-scale analysis to investigate how much of the response is dependent on the predominate frequencies contained in the earthquake record. A trace of the first 20 seconds of the Kobe earthquake is given in Figure 27. The PGA is 0.6g at 5.8s. The spectrum acceleration for this record is presented in Appendix G, the energy of the earthquake is

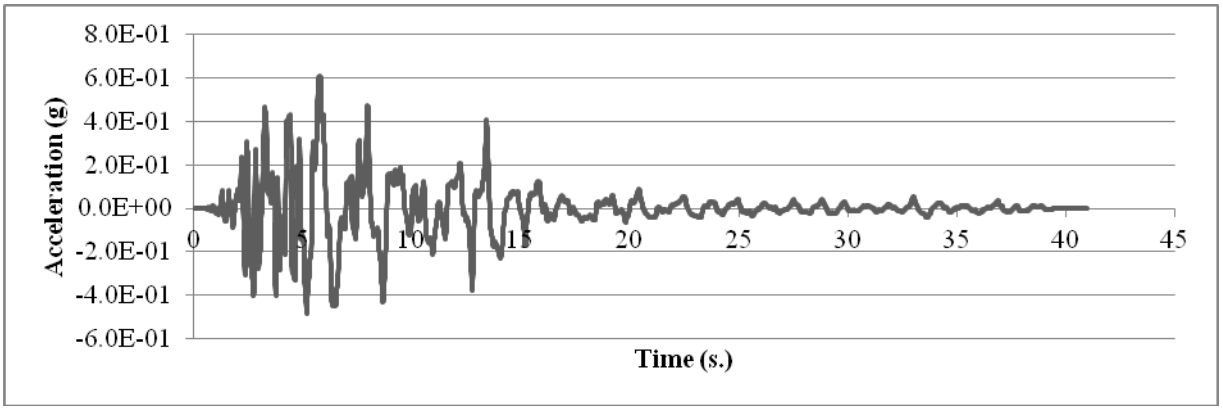

Figure 27: 1995 Kobe earthquake trace

transmitted at periods greater than 1s, which is closer to the natural period of the non-isolated configurations.

In the previous section, the reduction in terms of shear deformation was shown to be small between the different configurations of isolation. Only the non-isolated, the Isolation 1 and the Isolation 2 models were run with the Kobe earthquake. The same springs' stiffness and

coefficients of damping were used. The total displacements for the three models are shown in Figure 28. The non-isolated model has a maximum displacement of 1.17ft.

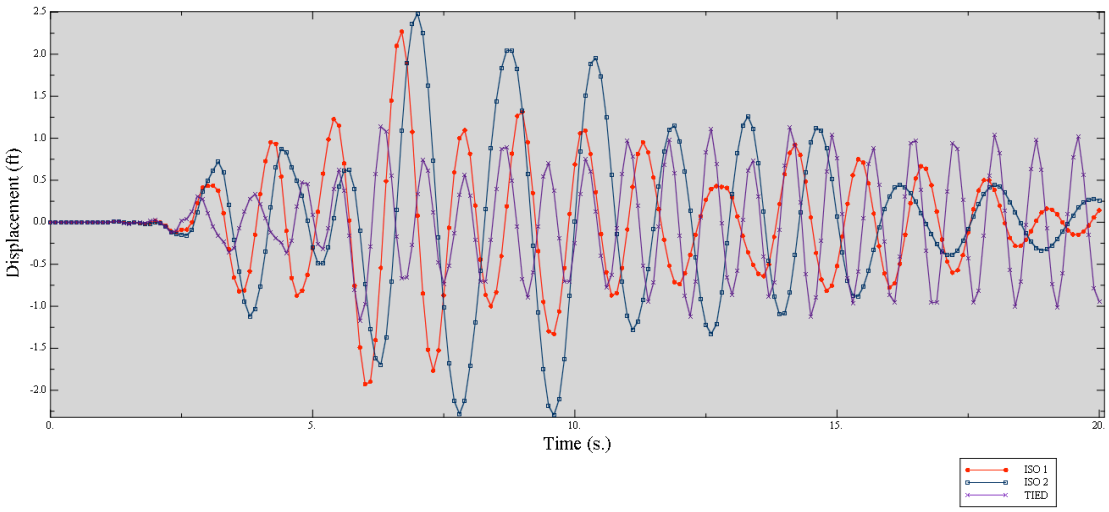

Figure 28: Building displacement under 20s. Kobe earthquake

As expected, the oscillations of the isolated models were more significant when compared to those predicted for the Canoga Park earthquake. The Kobe earthquake record contains much more power in frequencies closer to the frequency of the non-isolated model. The story accelerations are given in Appendix H. Without isolation, the upper story experiences a maximum acceleration of 2.1g. With the first story isolated, the acceleration at level 10 is 1.6g. Due to the addition of damping the isolated model reduced the top acceleration by a factor of almost 2 and brings the structure at rest faster. The panel deformation at maximum building displacement for the two models is shown in Figure 29.

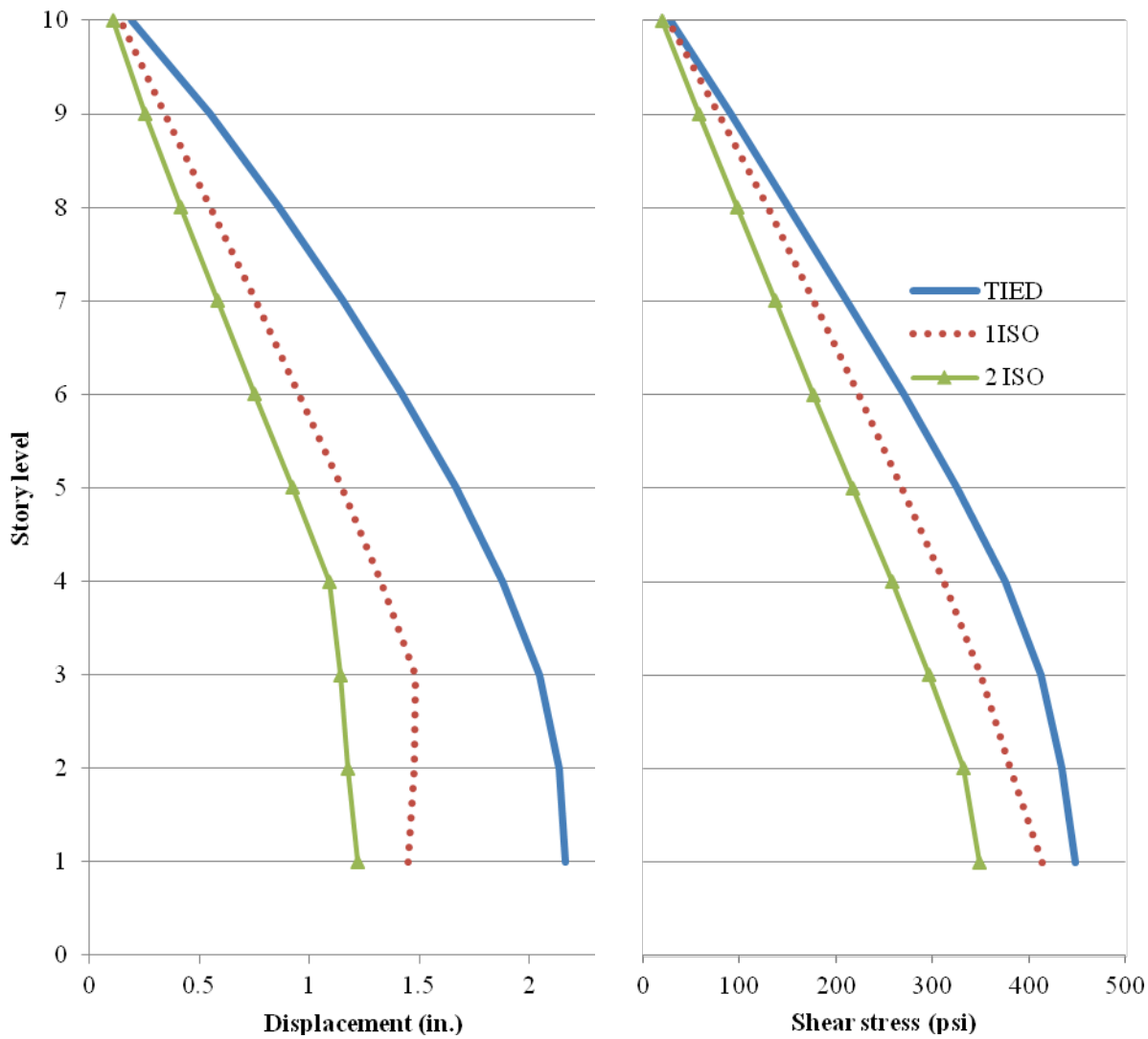

Figure 29: Panels deformation for Isolation 1 and non-isolated models at maximum building displacement

The reduction of panel deformation is less significant with the Kobe earthquake when isolating 1 or 2 stories compared to when the building is subjected to the Canoga Park earthquake. The averaged percentage reduction between Isolation 1 and non-isolation is just 32%. The notable difference is the wider gap between Isolation 1 and Isolation 2. This highlights the interest of increasing the natural period of the building by adding isolation levels. Taking the

natural period of the building away from the frequencies with the majority of power for the major earthquakes reduces the building response. With a ground motion excitation at a lower frequency, the reduction of panel deformation is less important, but the damping still has a notable effect on the acceleration and the energy dissipation, has shown in Appendix H. Considering the displacement capacity of the shear wall used in section VI-B of 1.5 in., a non-isolated structure would failed during the Kobe event. The deformation displacement is dropped below the safe point when isolating one or more stories.

In terms of demands on the isolators, activating more levels reduces the load on each element, as depicted in Figure 30. The slip displacement of Isolation 1 is above the limit of 0.5ft., which might be expected because the PGA of the Kobe earthquake is higher than the earthquake used to originally design the spring elements. The slip displacement is still in an acceptable range and the difference can assumed to be negligible.

VI. Conclusion

CLT has a promising future in tall building applications. The results confirmed the conclusions of Ryan & Earl (2010). The use of springs and dashpots to connect the first two stories together is the most effective system to reduce the seismic response. Adding isolators at higher level does not reduce significantly the seismic response. Nevertheless it allows minimizing the size of the isolators at each level. It also moves the structural response away from the range of periods with the predominate power for major earthquakes.

The stiffness of the springs has been selected to limit the slip displacement to ½ ft. The springs stiffness required to isolate 1, 2 or 3 stories is in the range of 10 kip/in to 40 kips/in. A reliable technique to estimate the amount of damping coefficient necessary has been presented. The damping coefficient to isolate 1, 2 or 3 stories is in the range of 1,700 to 28,000 slug/s.

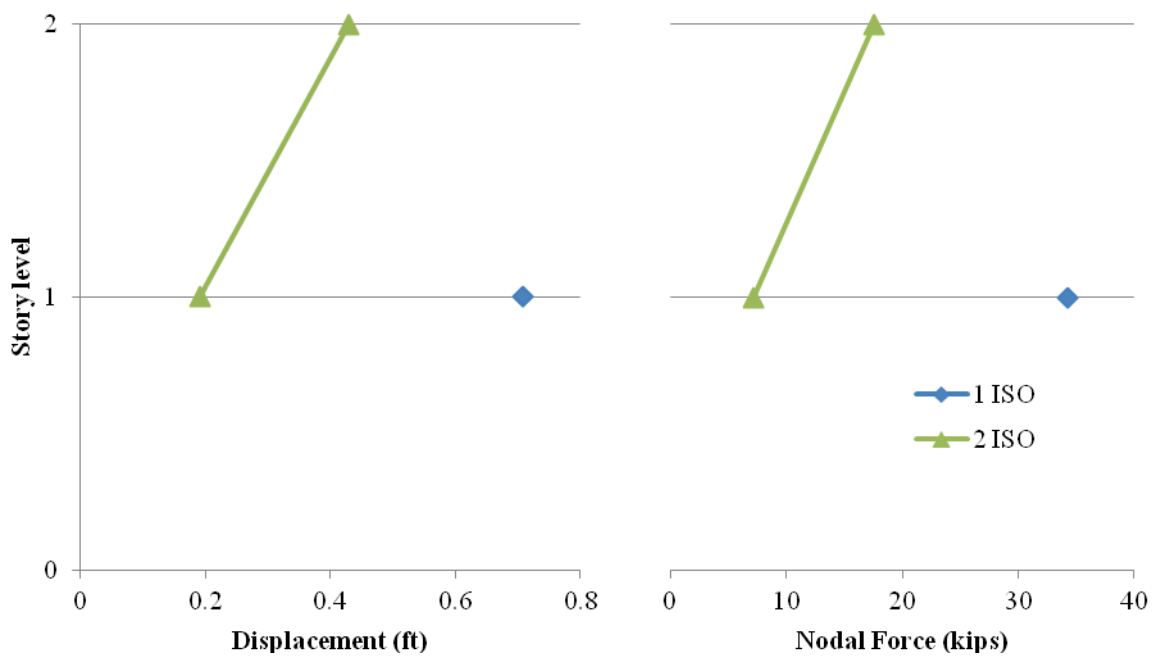

Figure 30: Slip displacement and nodal forces at dampers' connection at isolated levels

Depending on the earthquake input, the deformation of the panels could be reduced at least by 32%.

Distribute base isolation seems to be an effective technique to meet the requirements of seismic codes. But, a cost analysis must be done to investigate if the final price could let the construction of a CLT skyscraper in a seismic area possible.

VII. Bibliography

ASCE 7 (2010). "Minimum Design Loads for Buildings and Other Structures", ASCE/SEI Standards.

APA (2011). "Standard for Performance-Rated Cross-Laminated Timber" ANSI/APA PRG 320-2011.

Ceccotti, A., Sandhaas, C., & Yasumura, M. (2010). "Seismic Behavior of Multistory Cross-Laminated Timber Buildings" paper SD-1, Proceedings of the International Convention of Society of Wood Science and Technology and United Nations Economic Commission for Europe, Timber Committee, Geneva, Switzerland.

Filiatrault, A., & Folz, B. (2002). "Performance-Based Seismic Design of Wood framed Buildings" 128:1(39), *Journal of Structural Engineering*.

Filiatrault, A., Fischer, D., Folz, B., & Uang, C.-M. (2002). "Seismic Testing of Two-Story Woodframe House Influence of Wall Finish Materials" 128:1337-1345, *Journal of Structural Engineering*.

FPInnovation (2013). CLT Handbook.

Keunecke, D., Hering, S., & Niemz, P. (2008). "Three-Dimensional Elastic Behaviour of Common Yew and Norway Spruce" 42:633–647, *Springer-Verlag*.

Lauriola, M. P., Pinna, M., & Sandhaas, C. (n.d.). "Cyclic Tests on Cross-Laminated Wooden Panels" SOFIE Project, Italian National Research Council, Trees and Timber Institute San Michele all'Adige, Trento, Italy.

Lee, S. (2007). "Nonlinear Dynamic Earthquake Analysis of Skyscrapers by ABAQUS" 2007 ABAQUS Users' Conference.

Li, J., Li, Y.-C., Li, W., & Samali, B. (2013). “Development of adaptive seismic isoaltors for ultimate seismic protection of civil structures”, 1-12, Sensors and Smart Technologies for Civil, Mechanical, and Aerospace Systems.

Loferski, J. R. (1980). “Inelastic Stiffness Moduli for Nail Joints Between Wood Studs and Plywood Sheating” Oregon State University, Oregon, USA.

Marko, J., Thambiratnam, D., & Perera, N. (2006). “Study of Viscoelastic and Friction Damper Configurations in Medium-Rise Structures” 1(6):pp. 1001-1039, *Mathematical Sciences Publishers*, QUT.

Pei, S., Popovski, M., & Van de Lindt, J. W. (2012). “Seismic Design of a Multi-Story Cross Laminated Timber Building Based on Component Level Testing” World Conference on Timber Engineering., Auckland, August 2012.

Ramallo, J. J., Johnson, E. A., & Spencer, B. F. (2002). “"Smart" Base Isolation Systems” 128:10 (1088), *Journal of Engineering Mechanics*.

Ruan, S., Liang, Z., & Lee, G. C. (n.d.). “Animated Control of Structural Base Isolation System”, National Center For Earthquake Engineering Research, State University of New York ,Buffalo, U.S.A.

Ryan, K. L., & Earl, L. C. (2010). “Analysis and Design of Inter-Story Isolation Systems with Nonlinear Devices” 14: 1044–1062, *Journal of Earthquake Engineering*.

Skinner, R. I., & McVerry, G. H. (1975). “Base Isolation for Increased Earthquake Resistance of Buildings”, 93-101, *Bulletin of the New Zealand Society for Earthquake Engineering, Vol. 8*.

Skup, Z. (2001). “Structural Friction and Viscous damping in a Frictional Torsion Damper” , 497-511, *Journal of Theoretical and Applied Mechanics*.

Van De Kuilen, J. W., Ceccotti, A., Xia, Z., & He, M. (2011). “Very Tall Wooden Buildings with Cross Laminated Timber” 14: 1621–1628, *Elsevier Ltd*.

Vessby, J., Enquist, B., Petersson, H., & Alsmarker, T. (2009). “Experimental Study of Cross-Laminated Timber Wall Panels” 67: 211-218, *Springer-Verlag*.

VIII. Appendix

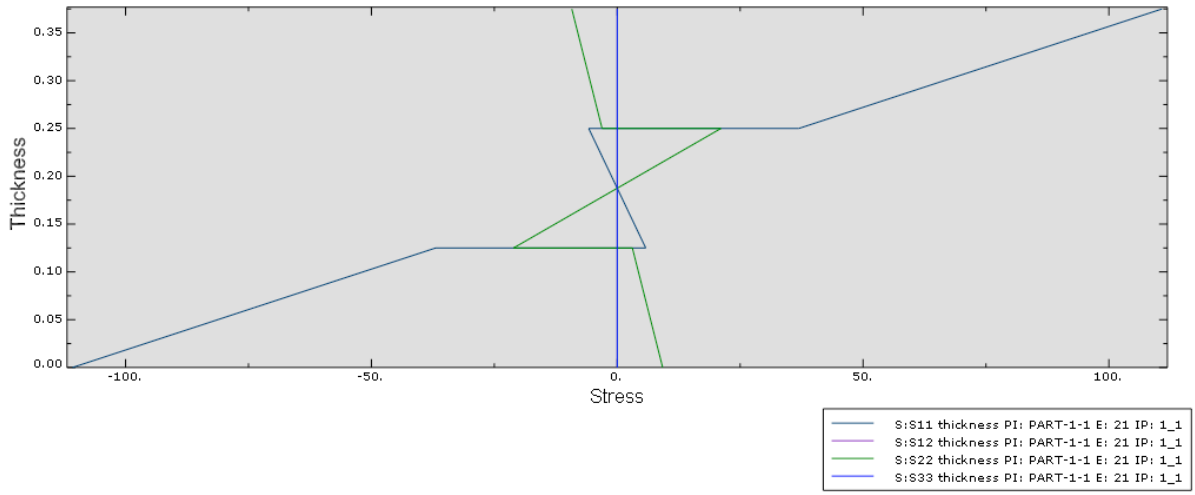

Appendix A: Shear stress in tensile test along the x-direction

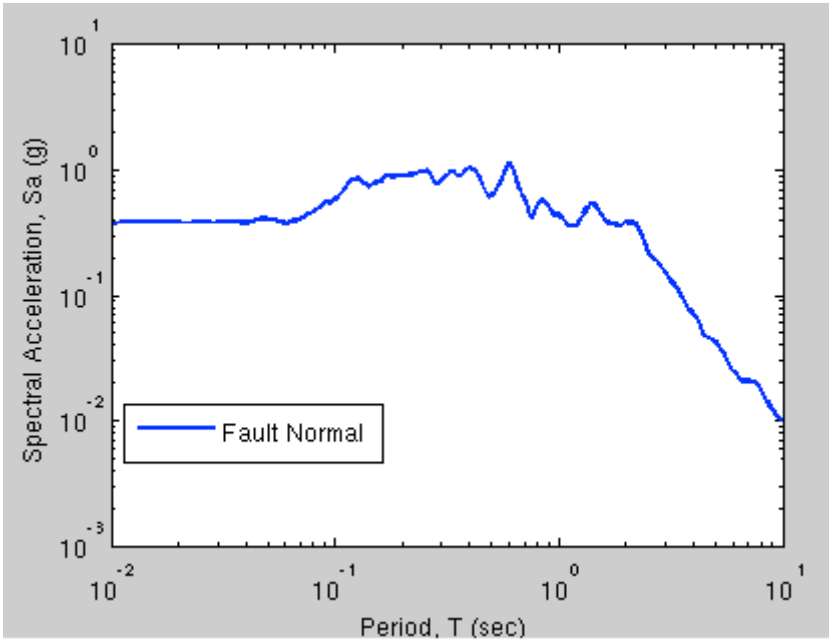

Appendix B: Canoga Park earthquake spectrum acceleration from PEER database

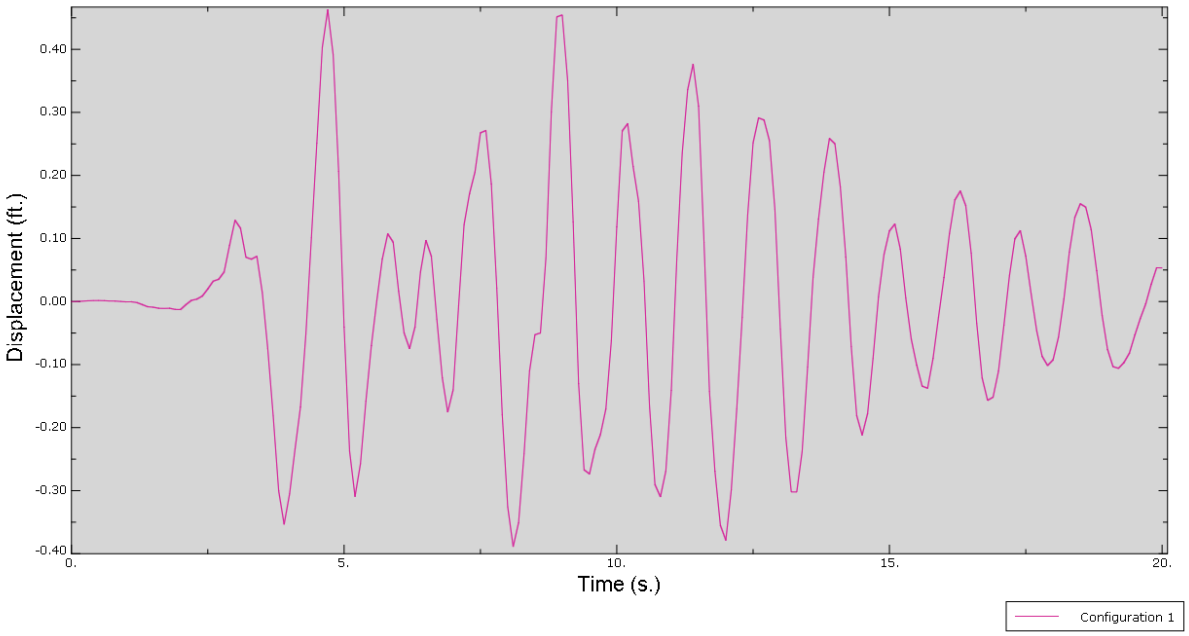

Appendix C: Building drift for Isolation 1 under Canoga Park excitation

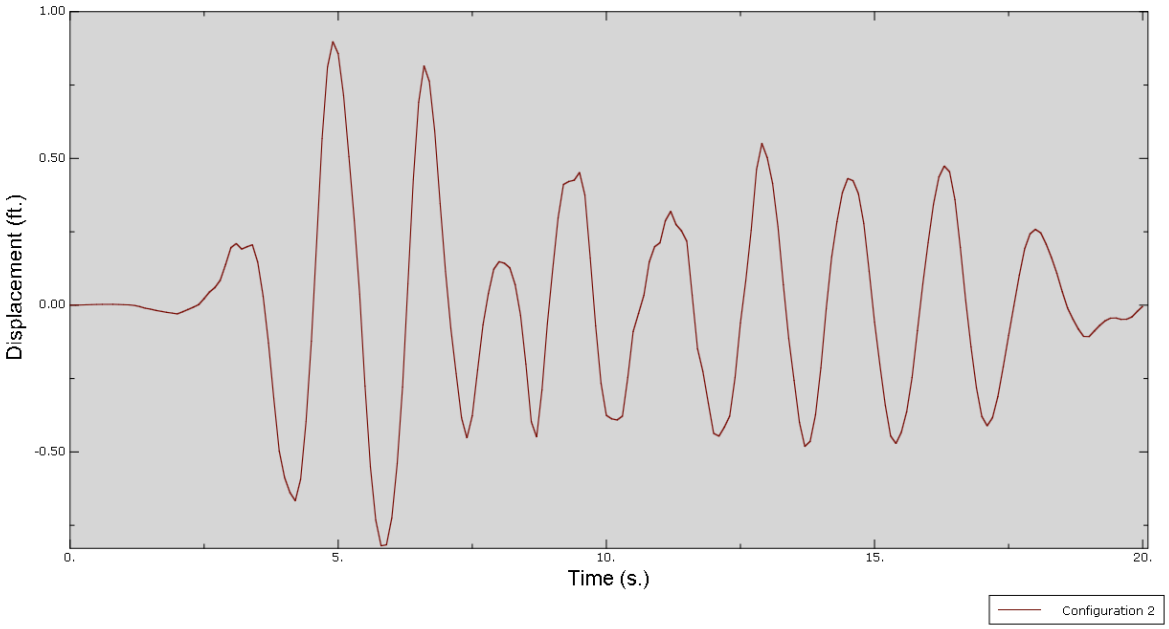

Appendix D: building drift for Isolation 2 under Canoga Park excitation

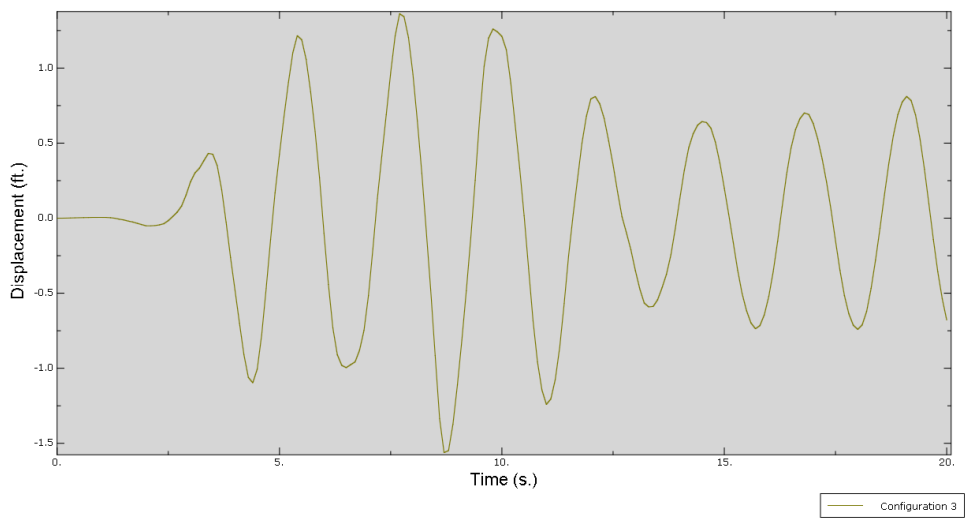

Appendix E: Building drift for Isolation 3 under Canoga Park excitation

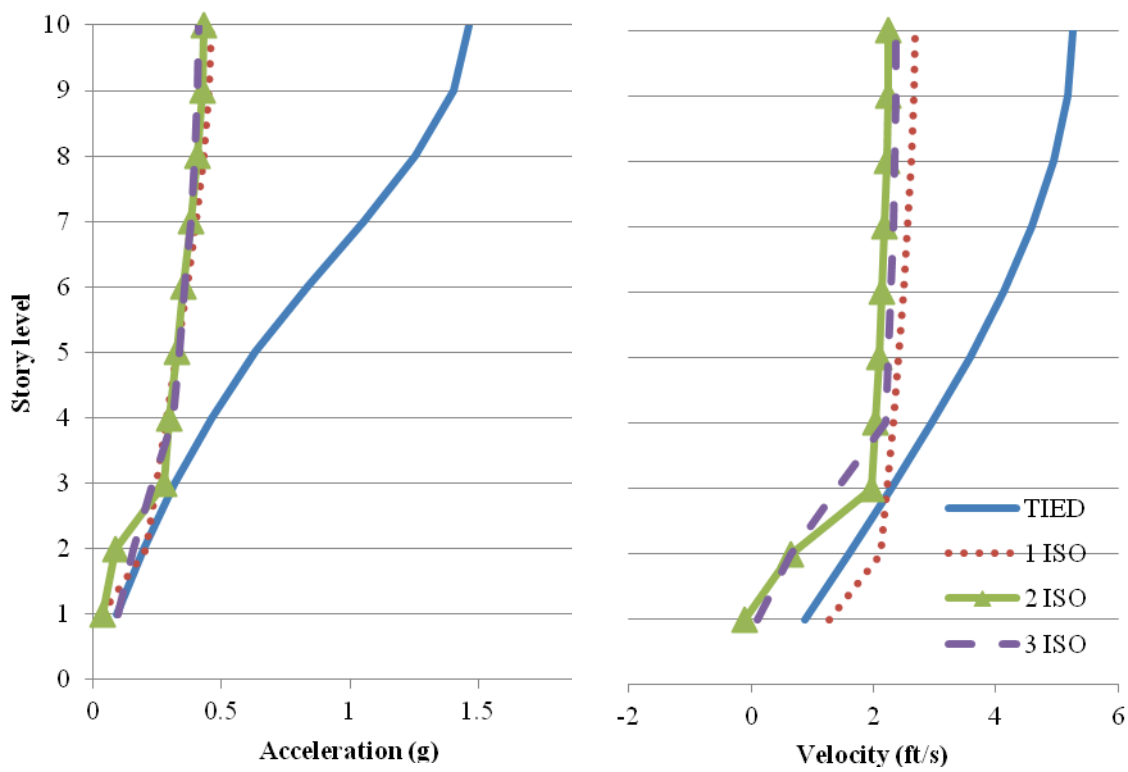

Appendix F: Acceleration and velocity profile at peak displacement for Canoga Park earthquake

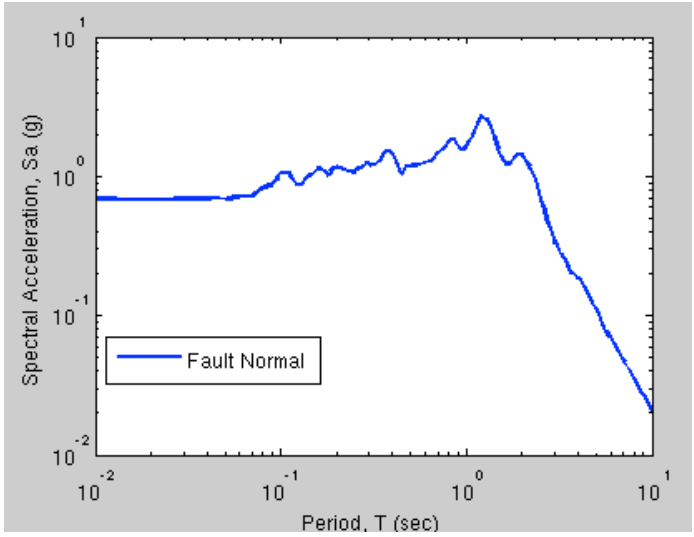

Appendix G: 1995 Kobe, Japan earthquake spectrum acceleration from PEER Ground Motion Database

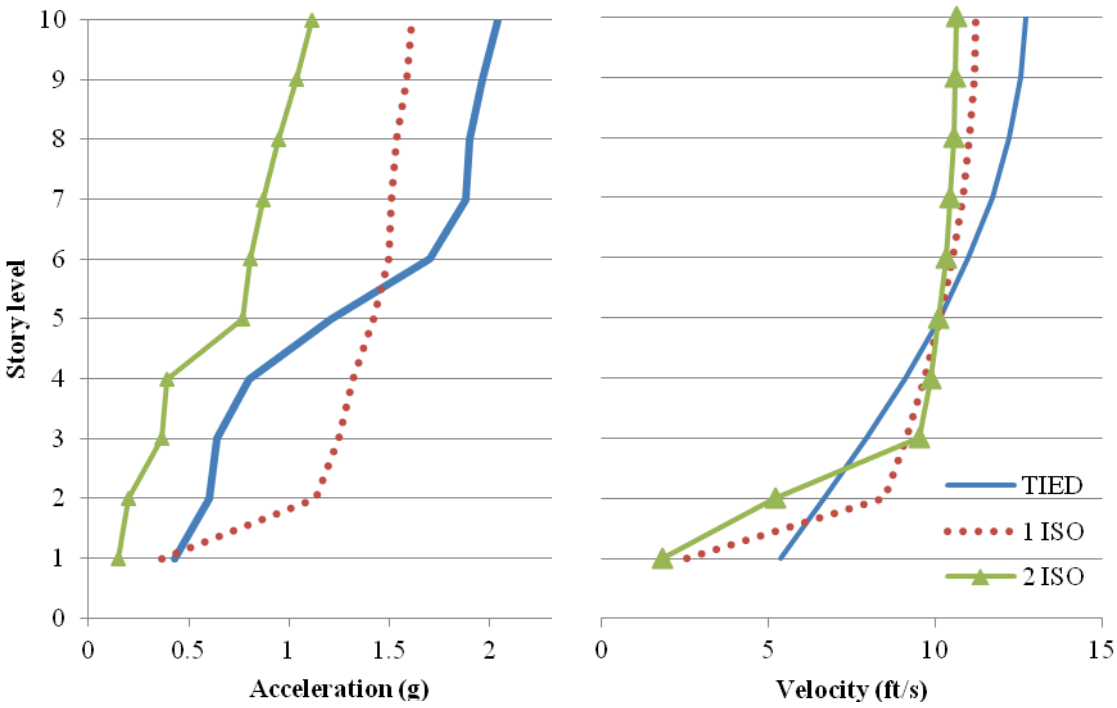

Appendix H: Acceleration and velocity at maximum drift for Kobe earthquake